# Computer Simulation of the Effects of Muscle Co-activation and Joint Stiffness on Postural Stability

A Thesis Submitted to the

College of Graduate Studies and Research

in Partial Fulfillment of the Requirements

for the degree of Master of Science

in the Department of Computer Science

University of Saskatchewan

Saskatoon

By

Mohammad Shabani

# Permission to Use

In presenting this thesis in partial fulfilment of the requirements for a Postgraduate degree from the University of Saskatchewan, I agree that the Libraries of this University may make it freely available for inspection. I further agree that permission for copying of this thesis in any manner, in whole or in part, for scholarly purposes may be granted by the professor or professors who supervised my thesis work or, in their absence, by the Head of the Department or the Dean of the College in which my thesis work was done. It is understood that any copying or publication or use of this thesis or parts thereof for financial gain shall not be allowed without my written permission. It is also understood that due recognition shall be given to me and to the University of Saskatchewan in any scholarly use which may be made of any material in my thesis.

Requests for permission to copy or to make other use of material in this thesis in whole or part should be addressed to:

Head of the Department of Computer Science

176 Thorvaldson Building

110 Science Place

University of Saskatchewan

Saskatoon, Saskatchewan

Canada

S7N 5C9

# Abstract

Postural stability is affected by several biomechanical factors including posture, foot placement, intrinsic muscle stiffness, and joint stiffness due to muscle co-activation. Increasing natural postural stability could make balance control easier for individuals with diminished postural responses. However, it is not clear which biomechanical factors most significantly contribute to the natural postural stability. The objective of this thesis is to simulate the effect of intrinsic muscle stiffness and muscle co-activation on the postural stability using a musculoskeletal computer model subjected to support-platform perturbations. We developed a customized static-optimization method to encourage co-activation using joint stiffness as an intermediate variable to improve postural stability. To this end, we also implemented a short-range stiffness muscle model and compared its stabilizing effects to a standard Hill-type muscle model. Our result showed that co-activation of muscles resulted in higher joint stiffness and higher postural stability and that intrinsic muscle short-range stiffness contributed significantly to postural stability.

# ACKNOWLEDGEMENTS

# CONTENTS

# LIST OF TABLES

# LIST OF FIGURES

# LIST OF ABBREVIATIONS

| | |
|---|---|
| SRS | Short Range Stiffness |
| 3D | Three Dimensional |
| DOF | Degrees of Freedom |
| GUI | Graphical User Interface |
| API | Application Program Interface |
| ID | Inverse Dynamics |
| GRF | Ground Reaction Force |
| CMA | Covariance Matrix Adaptation |
| BFGS | Broyden-Fletcher-Goldfarb-Shanno |
| FD | Forward Dynamics |
| HCF | Hunt Crossley Force |
| COM | Centre of Mass |
| COP | Center of Pressure |
| BOS | Boundary of Support |
| Tib-Ant | Tibialis Anterior |
| Med-Gas | Medial Gastrocnemius |
| Vas-Int | Vastus Intermedius |
| Rect-Fem | Rectus Femoris |
| Psoas | Psoas Major |
| Sar | Sartorius |
| Bifemsh | Short Head Biceps Femoris |
| Bifemlh | Long Head Biceps Femoris |
| LBFGS | Limited-memory Broyden-Fletcher-Goldfarb-Shanno |
| EMG | Electromyography |
| MSE | Mean Square Error |
| Biceps-Short | Short Head Biceps Brachii |
| Biceps-Long | Long Head Biceps Brachii |
| BRA | Brachioradialis |
| TRI-Long | Long Head Triceps Brachii |
| TRI-Lat | Lateral Head Triceps Brachii |
| TRI-Med | Medial Head Triceps Brachii |
| MPE | Mean Percentage Error |
| OS | Overall Stability |

# Chapter 1

# Introduction

Attempts to understand and describe physical mechanics of the human body through computer simulation have become one of the most interesting and challenging areas in the past decades. Biomechanical models supply tools to analyze movement and forces in a complex system. Employing computer software provides ability to study the biomechanics of the body in a safe simulation environment. Besides, it provides possibility to perform a large number of simulated experiments in a short time. These benefits led to a high demand for simulators and nowadays, there are dozens of software toolkits available for simulation such as OpenSim, ArtiSynth, FEBio, etc. These simulators provide facilities to analyze a variety of biomechanical tasks like gait, jumping, or standing. Standing balance is one of the biomechanical demands that the human body should be able to perform perfectly for many different daily movements. Failure to stand or walk with good stability can lead to falls and, in turn, bone fractures.

The stability of the body has two main contributors: natural (or intrinsic) stability and active responses from the central nervous system. These two components of stability have a distinct effect on postural stability. Depending on the posture of the body and external stimuli, one component can become more important compared to the other. The bodys intrinsic stability becomes more important when ones reflex and active posture responses to external perturbations are delayed or diminished, and can partly compensate for diminished reactions to maintain balance. In such a case, higher intrinsic stability can lead to less need for feedback responses. The intrinsic stability of the human body is affected by different biomechanical factors, such as muscle stiffness, muscle co-activation, body posture, etc., but the degree to which these factors can affect the bodys intrinsic stability is unclear.

This thesis describes the development and evaluation of new computer simulation tools that help to describe the relationship between muscle co-activation and joint stiffness estimated from the intrinsic Short Range Stiffness (SRS) of muscle tissue and the effect of joint stiffness on postural stability. In this thesis, we develop a new static optimization formulation that uses a target joint stiffness to elicit co-activated muscle recruitment. We also developed a new muscle model to capture intrinsic SRS of the muscle, which leads to more accurate joint stiffness. Furthermore, we implemented a feature into OpenSim to measure joint stiffness. Finally, we performed posture simulations to investigate the effect of co-activation and SRS of the muscle on posture balance. The degree to which the muscle co-activation and SRS can increase postural stability, however, is an open question; therefore, our objective is to use biomechanical simulations to quantify the

1

increase in postural stability that is achieved by the co-activation and SRS.

## 1.1   Motivation

Maintaining balance while standing and walking is typically accomplished with ease and taken for granted by most healthy individuals. In contrast, diminished balance control, which is prevalent among adults over the age of 65, poses a significant health concern that is reflected in a much higher rate of fall-related injury [19]. Falls among older adults may be caused by several reasons, such as muscle weakness (particularly in the legs), poor balance control, sensory problems, reflex problems, etc. These problems subsequently lead to serious injuries and make the person, who is affected, less likely to be independent. For example, falls are responsible for over 95% of hip fractures [49]. Due to higher rate of falls in seniors in comparison to the younger people [65], it becomes more important to focus on old aged group and find strategies that could decrease the fall rate in older adults.

Falls and fall-related fractures in older adults is a growing concern as the median population age rises [42]. In 2010, eight per cent of the world population (about 524 million people) was 65 years old or above and this number was predicted to triple by 2050 [46]. Older adult population (aged 65 or older) is predicted to outnumber children aged 5 years old or below in the next few years [45]. While the total population growth rate decreased in past decades, older people population increased significantly [44]. Owing to better educations, sanitation, nutrition status, and comprehensive health care in developed countries, people live significantly longer. Accordingly, the old population growth rate is higher in these countries compared to developing countries [61]. In line with this, the Canadian population is also aging fast. The older population is predicted to be 24.7% of the total population in 2051 [41]. Figure 1.1 demonstrates that since 1975 there has been a marked decrease in the world population growth rate, while the population of older adults started to increase. It is predicted that this number reaches a peak between 2025 and 2030.

A larger population of older adults, which is associated with higher risk of falling, can lead to some major problems. Though, bone fractures and serious brain injuries frequently happen in the older adults, which can also lead to death. It has been report that the type of the injury associated with a fall can vary from one age group to another [65]. They report more often injuries to knee and head in the older group. Each year, millions of people receive medical treatments due to age related falls and the cost of treating goes up with age [18, 64].

Average cost for fall related injury, for each person, is reported to be $35,000 (in 2006) and it is among one of the 20 most expensive medical treatments [7]. Canadian health care costs are predicted to rise to more than $2.4 billion by 2041 [68]. In 2013, 1-year incremental healthcare costs for fall-related fractures were estimated at $137 million for women and $57 million for men [32]. Fall-related fractures among older adults not only increase health care costs, but are also associated with great pain and morbidity for individuals afflicted [43] [53].
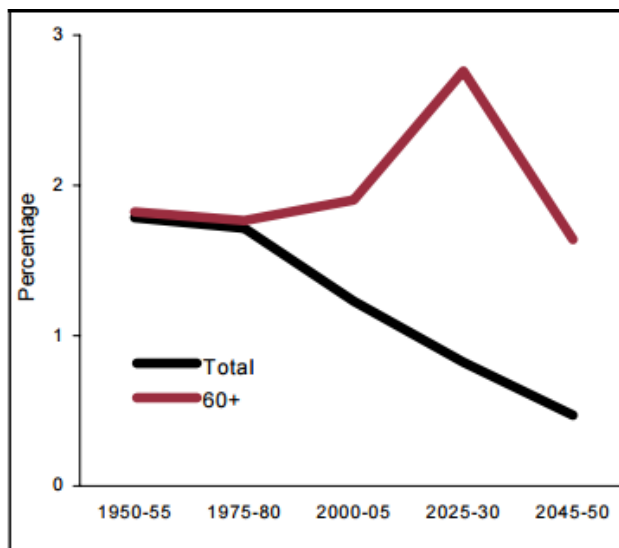
**Figure 1.1:** Average annual growth rate of total population and population aged 60 or above. World total population growth rate has started to decrease since 1975-80, while the population of older adults are having an increasing growth rate. The image is taken from [44]

It is not surprising that a fall in an older adult could lead to serious injuries and pain, but it also could lead to fear of falling. There is a significant correlation between a previous fall and fear of falling in older adults. This fear of falling can be prevented for better life quality in those people suffering from [57]. Aside from the injuries and pain, healing time for older adults suffering from a bone fracture, caused by a fall, is extremely long.

The increasing population of older adults and higher risk of falls in this group can cause both social health care and personal costs. Unfortunately, balance treatment programs are commonly initiated once an individual has experienced a fall. Therefore, new methods for improving balance, before a fall occurs, are needed. Improvement of natural postural stability can improve balance and reduce the risk of a fall.

Investigating ways to improve balance and postural stability in individuals using experimental measurement alone makes it difficult to assess the relative importance of the various biomechanical factors that affect postural stability. Some of these factors, such as joint stiffness, are not available for direct measurement. Therefore, those parameters should be measured indirectly. Also, using a simulation environment, it is feasible to change one factor while keeping the rest of the factors constant. But, this approach is not possible in a study with human participant. Moreover, during a human participant experiment the participant's safety is paramount. Support platform perturbation is a common experimental setup for assessing stability [27], but large perturbations that make the participant fall could be unsafe for human participants. Simulating perturbations with a Three Dimensional (3D) musculoskeletal computer model avoids safety concerns and allows us to manipulate biomechanical factors, such as intrinsic muscle stiffness and muscle co-activation, and assess their relative importance to stance stability.

It is feasible to improve a variety of factors to elevate postural stability. In this regard, highlighting muscle

recruitment and encouraging muscle co-activation are some potential possibilities. Muscle co-activation is a phenomenon in which a muscle is activated accordingly with its opposing muscle. For instance, knee has two groups of muscles: knee flexors and knee extensors. Co-activation happens when both groups are activated at the same time for an specific tasks. The knee flexors are activated when a person intends to flex his/her knee. This group is called agonist muscles in this task. The opposing group for this task, extensors, are called antagonist muscles. Higher agonist and antagonist muscle activations may improve stability of stance by increasing the stiffness of joints and stabilizing them.

## 1.2 Problem

Our hypothesis is that higher muscle co-activation and joint stiffness, estimated from muscle stiffness, will lead to higher postural stability. We can evaluate this hypothesis with computer simulation, but there are a number of technical problems that need to be addressed in order to create simulations:

1. Simulation techniques for muscle recruitment commonly employ optimization to spread joint torques among multiple redundant muscles [17]. A common optimization criterion is minimization of muscle forces or activations, but this also minimizes co-activation, as it spreads forces among agonist muscles and minimizes activations of antagonists. Therefore, a new set of formula should be implemented to encourage co-activation.

2. Accurate measurement of muscle stiffness plays a crucial role in the estimation of a joint stiffness. Recent works have demonstrated that Hill-type muscle models result in a remarkable underestimation of stiffness of the arm and knee [28, 52]. However, this model is one of the most accurate and precise models for muscle and is highly tested and widely used in different simulation software such as OpenSim and Artisynth [14, 35]. In a static equilibrium, muscle stiffness is dominated by the SRS and therefore joint stiffness can be directly estimated from SRS of muscles, which is proportional to the muscle force and inverse of the muscle optimal fiber length [12]. Therefore, a new muscle model is necessary to capture the intrinsic SRS. The SRS has not yet been incorporated in forward dynamics simulations ( e.g. to investigate the effect of the SRS on postural stability). However, recent studies have used SRS to map muscle stiffness to joint stiffness [28, 52].

3. OpenSim provides facilities to measure a variety of parameters in a model, which would be hard or nearly impossible to measure directly in an experiment; OpenSim does not provide a built-in way to measure joint stiffness. Consequently, a new technique to measure the joint stiffness seems to be necessary.

4. There is a need for a simulation environment to execute simulations of support platform perturbations for systematically testing postural stability for different levels of muscle co-activation and joint stiffness.

This simulation should provide a proper way to examine the stability of the model and compare it to the stability of other model setups.

## 1.3 Solution

In this section, we will describe our solutions for the problems, which are mentioned, in order to test our hypothesis. Each problem is addressed in this section briefly, and then with complete details and results in the next chapters.

1. Several studies focused on an objective function selection and tested the output's sensitivity based on the objective function and parameters selection [3, 24, 10, 21]. Additionally, a few investigations have been done to make the optimization more computationally efficient by selecting a linear objective function and converting the problem to a linear problem. [55, 50]. A few select approaches have performed static optimization while allowing co-activation, including separate optimization for flexor and extensor muscle groups [52]. These previous approaches, to simulate co-activation, require a direct prescription of the degree of co-activation; however, it would be better to allow co-activation to arise naturally based on a related physiological parameter. To address this problem, we used joint stiffness as an intermediate variable, in our new optimization formulation, to let the muscles freely choose activations by setting a target stiffness at a desired joint. Increasing the stiffness of the joint would result in higher activations of agonist and antagonist muscles which are associated with that specific joint. Using this technique, we performed optimizations on a range of stiffnesses at the target joint (knee). To estimate the target joint stiffness, we used muscle stiffness and mapped stiffness of muscles, which are related to the corresponding joint, to the joint stiffness.

2. To overcome the second problem, we developed a new *SRSMuscle* model (*SRSMuscle*) in OpenSim. The *SRSMuscle* model is an extension to *PathSpring* — a spring, which can path two or more points — and the stiffness of this model is represented as SRS of the muscle [52]. This implementation provides the ability to estimate, accurately, the stiffness of the joint from the muscle stiffness. Joint stiffness is especially important in static equilibrium and is mostly dominated by muscle SRS in this situation. We evaluated stiffness produced by the *SRSMuscle* model by comparing knee stiffness to experimental data. SRS model is used to estimate joint stiffness in new technique for static equilibrium optimization which makes it possible to have controlled level of co-activation in muscles. This is especially important because the methods employed by others for optimization do not allow activation at all or with certain constraints. The new *SRSMuscle* model, which is developed in OpenSim, also allows to integrate SRS in our posture perturbation simulations.

3. Joint stiffness is defined as the ratio between a small change in applied torque at a joint and a small displacement of that joint. It states the extent to which the joint can resist in response to an applied

force. There are two approaches that can be used to measure the joint stiffness. In the first approach, the analytical approach, the relationship between applied toques to the joint and its stiffness, could be expanded to an equation that relates the stiffness of the joint to a set of applied forces, moment arms, and moment arm derivatives. The second approach, to measure the joint stiffness, is to calculate the partial derivative of the joint with respect to its coordinate, numerically. This approach is not as fast as the first approach, but does not need moment arms and moment arm derivatives as direct inputs. Hence, in a situation, when the moment arm derivatives are unknown, this approach could be convenient way to measure the joint stiffness.

4. Although employing static-optimization to achieve co-activation with a *SRSMuscle* model solves the underestimated stiffness problem of Hill-type muscle and provides ability to accurately estimate the joint stiffness, a new simulation setup is necessary to study the effect of different levels of co-activation on postural stability. We employed posture perturbation setup and modified it to match our study [58]. First, we added new controls for the *SRSMuscle* model to be able to simulate both posture models (model with the Hill-type muscles and the *SRSMuscles*). We also created a new storage to collect data, such as model states, forces, torques, and etc., from simulations, and put data in corresponding directories. At the end, we created bash scripts to run desired simulations automatically.

## 1.4 Contributions

The main contributions of this thesis are:

1. Design and implementation of a new technique for optimization that allows co-activation of agonist and antagonist muscles together based on a target joint stiffness. The new static optimization formulation is evaluated by investigating the convergence of the cost function. Optimizer converges by satisfying the constraints and convergence tolerance.

2. Implementation and utilization of the *SRSMuscle* model in optimization and forward simulation. The stiffness of the *SRSMuscle* is compared to experimental data over a range of knee extension torque. Experimental data for the knee stiffness is reported versus knee extension torque [52]. Therefore, we selected a range of torque values for the knee extension, and for each torque value, we performed an optimization to find minimum activations that are needed to produce such a torque. The knee stiffness, which was calculated based on these activations, is compared to experimental data.

3. Implementation and evaluation of two methods (numerical and analytical) to measure joint stiffness for a musculoskeletal model in OpenSim. These approaches are tested and verified with different force models including bushing force, spring, and Hill-type muscle.

4. Simulation-based analysis of posture stability. We evaluated the stability of Hill-type and *SRSMuscle* models with 16 co-activation (and force) levels using a perturbation-based simulation environment.

The stability of stability of the different model configurations was compared to determine the effect of co-activation and muscle stiffness on postural stability.

## 1.5   Thesis Outline

In this section, we will describe the overview of the thesis. This thesis is arranged in six chapters. Current chapter, Chapter 1, described the main motivation for this work, and problems that should be addressed. Furthermore, possible solutions and main contributions of this thesis were explained.

- Chapter 2 presents background information on topics that are necessary for the understanding of the following chapters of this thesis. This includes description of the different biomechanical models including muscles, bones and joints. This chapter also covers a background on the stability of the body, as well as simulation techniques (inverse/forward dynamics and static optimization).

- Chapter 3 is designated to cover new optimization formulation and its results. A new technique to measure the joint stiffness, in OpenSim, is described and tested with different force models. The limitations of the new static-optimization technique are also discussed in this chapter.

- Chapter 4 describes the SRS model, the reason for its necessity, and the way in which it can be integrated into OpenSim and forward simulations. We provided a detailed description that explains the benefits that our work can gain from using *SRSMuscle*. The *SRSMuscle* model is implemented and employed in optimization and forward simulations.

- Chapter 5 describes our simulations of postural stability with different model configurations. This chapter provides details of our technique, to measure overall stability of a model configuration, by perturbing the support platform beneath the model. The effect of co-activation on the postural stability and the degree in which the *SRSMuscle* or Hill-type muscle can be integrated to standing stability, is investigated.

- Chapter 6 provides a summary of the thesis. It presents the main contributions of the thesis, limitations of the work, and directions for future work that can improve the result of this thesis.

# CHAPTER 2

# BACKGROUND

This chapter focuses on novel computer simulation techniques that are applied to analyze postural stability. In this chapter, we provide background on computer simulation of musculoskeletal systems. Section 2.1 describes model structure in OpenSim and the model we employed for this thesis. Section 2.2 will include inverse and forward dynamics as well as static optimization. The last section of this chapter (section 2.3) provides background on stability of stance and several factors that can affect it.

## 2.1 Lower Extremity Model

The lower limb model is a well-designed and validated model that is available to be employed in different studies in OpenSim (Figure 2.1). It is available in the OpenSim package under the name of gait2354 (23 refers to the number of DOFs of the model and 54 refers to the number of muscles). This model is a modified and improved version of [15] which is introduced to describe a lower extremity model based on experimental measurement and has corrected several known inaccuracies. The model enables simulation of lower limb and accurate examination of hip, knee, and ankle joints. The model has 19 degrees of freedom for the hip, knee, ankle, and subtalar joints. To produce joint torques, the model includes 54 Hill-type lower extremity muscles [39].

The skeleton of the model includes rigid bodies that represent the pelvis, femur, patella, tibia, fibula, talus, calcaneus, metatarsals, and phalanges bones. Joints of the model are custom joint which is the most generic joint model implemented in OpenSim. This joint provides 3 rotational coordinates as well as 3 translational coordinates. Contact point of pelvis and femur makes hip joint. Six muscle groups are responsible for hip joint movements including adduction, abduction, flexion, extension, internal rotation, and external rotations to provide 3 rotational movements to the hip. The knee joint is also a custom joint and provides one rotational coordinate. Two muscle groups knee extension and knee flexion are responsible for knee movements. The ankle also provides two types of movements, flexion/extension and internal rotation/external rotations.

The model has 54 Hill-type muscles divided into different groups to provide force actuation to the model. Appendix A provides detailed information about each muscle in the model. There are two limit forces to keep the movement of the knee and lumbar extension coordinates within a physiological range and prevent these coordinates from further movements. Hunt Crossley Force (HCF) model is used to represent contact between
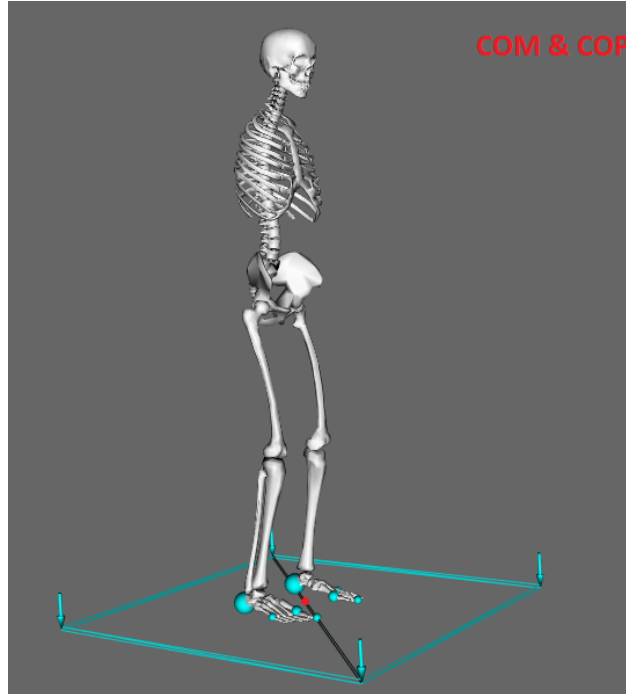
**Figure 2.1:** Lower extremity model was used for this thesis along with Support platform (cyan rectangle) and contact geometries (cyan spheres). The model's posture was configured in such a way that the centre of mass (COM) and centre of pressure (COP) was initially aligned to the centroid of the base of support

each foot and the ground. Two bushing forces are implemented at the knee and back. The non-muscle forces are controlled by parameters provided as part of the model. However, the amount of force generated by each muscle is controllable by the amount of activation supplied to the muscle. This model was employed to run the examinations in OpenSim for this thesis.

Figure 2.2 shows the model with 9 selected muscles. Among all 27 muscles in the one side of the model, we opted to present these muscles, because these muscles are highly affected by stiffness based optimization and were activated more than 10% at the highest level of target stiffness.

## 2.2 OpenSim

This section introduces common tools in OpenSim and the way in which those are used in this thesis.

### 2.2.1 Software Overview

OpenSim is an open source, user extensible software system for biomechanical modeling, simulations, and analysis that enables a wide range of studies [14]. It was developed at the Simbios center at Stanford University and released in 2007. Since then, it has been upgraded in several releases allowing users to employ it in different areas of studies such as rehabilitation, orthopedics, ergonomics, and robotics. OpenSim
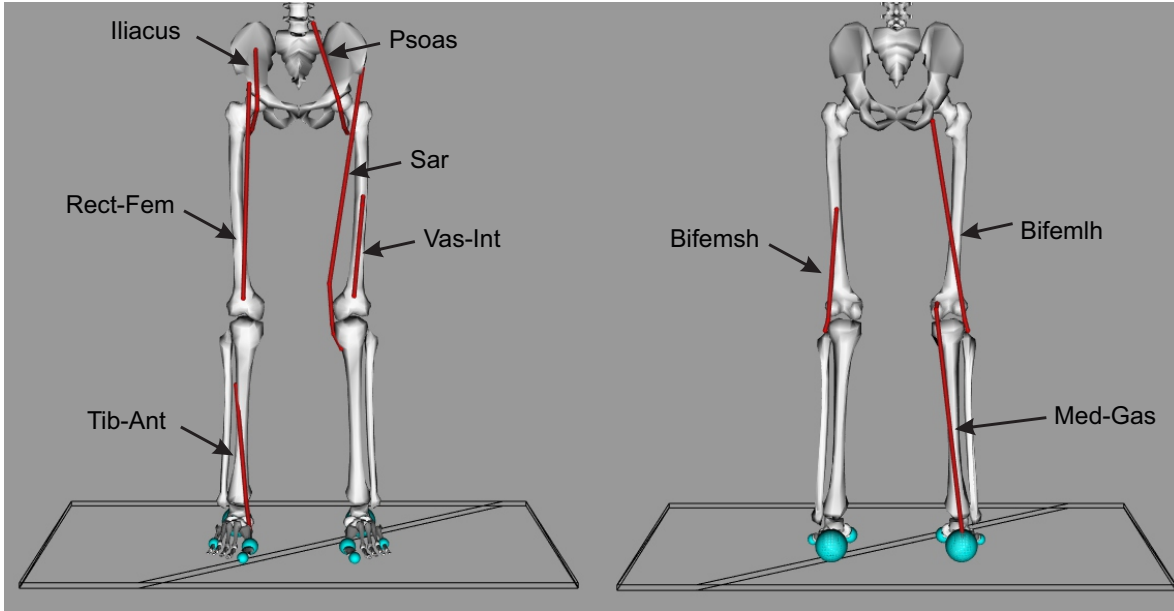
**Figure 2.2:** Nine muscles of the model are shown in the Figure: Tibialis Anterior (Tib-Ant), Medial Gastrocnemius (Med-Gas), Vastus Intermedius (Vas-Int), Rectus Femoris (Rect-Fem), Psoas Major (Psoas), Sartorius (Sar), Short Head of Biceps Femoris (Bifemsh), Long Head of Biceps Femoris (Bifemlh).

includes a number of musculoskeletal models that have been developed and shared by different research groups. These include an arm model [26], lower extremity models [15], shoulder model (MaBas et al. in prep), and lumbar spine model [8]. Unlike other simulators that use full coordinate representations (e.g. ArtiSynth) in which each rigid body gets 6 Degrees of Freedom (DOF) and extra constraint equations are added for joints, OpenSim uses internal coordinates for modeling which means each joint gets a certain number of DOF defined by the user and other DOFs for that joint are constrained by default [59].

In an OpenSim model, there is one rigid body for the root of the model and the rest of the rigid bodies are children and can be parents for other components. This means each component can have a child or children, but will only have one parent component. Therefore, an OpenSim model form a directed acyclic graph. Figure 2.3 shows the tree structure for the lower extremity model used in this thesis.

In a broad view, OpenSim is beneficial in identifying cause-effect relationships, visualizing complex movement patterns, and probe parameters that are hard to measure. In OpenSim, one can identify the cause of an event and its effect on the overall system. For example, one can manipulate the model to see factors that cause a crouched gait, and by the means of simulation, it is possible to evaluate its effect on gait. (Three Dimensional (3D) visualization of a simulation can be done by using the OpenSim's Graphical User Interface (GUI) written in *Java*. OpenSim also provides probes to measure different parameters during a simulation.

Furthermore, OpenSim provides tools for forward and inverse dynamics with robust optimization algorithms as well as powerful tools for simulations such as integrators. The OpenSim GUI is written in *Java* and provides access to features such as inverse and forward dynamic simulation and static optimizations
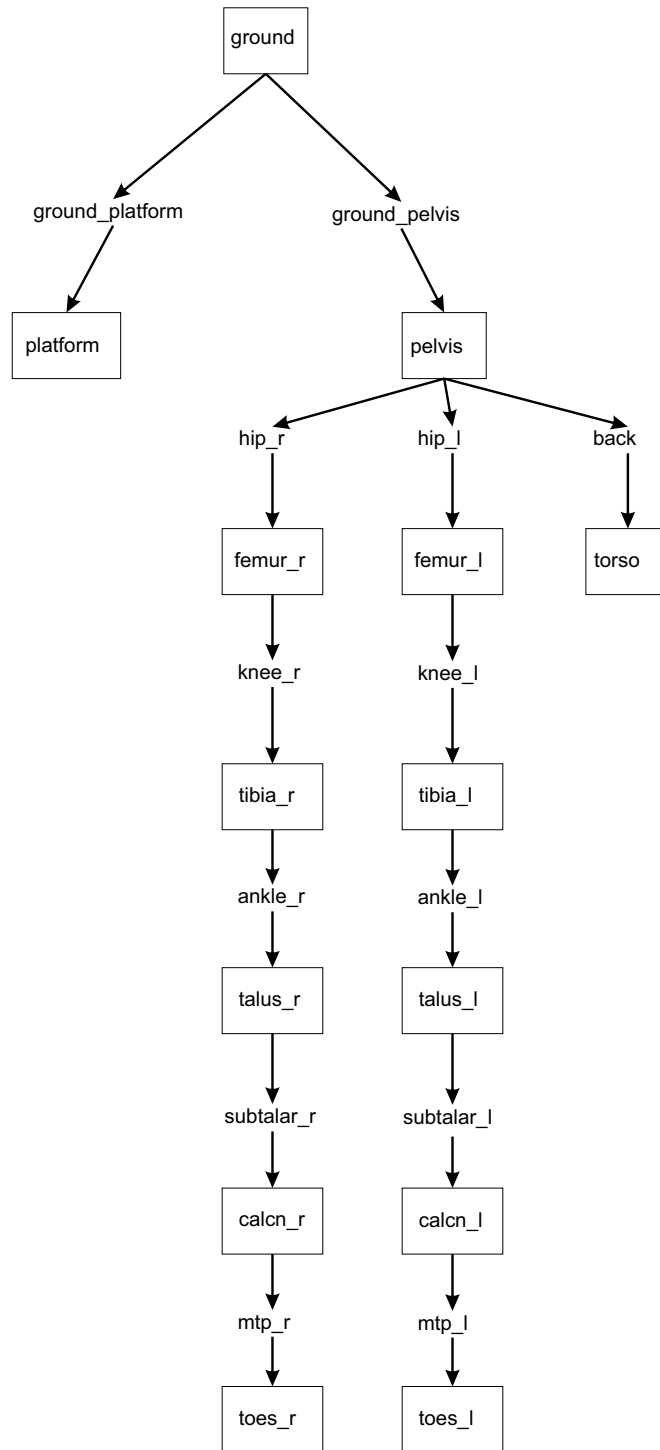
**Figure 2.3:** Topological view of the lower extremity model in OpenSim. Ground is the root of the model and parent to two other rigid bodies (platform and pelvis). Each node, in the tree, represents a rigid body in the model. Each edge in the tree represents a joint.

to run and analyze simulations. There is also a plotter that enables users to plot a variety of data from the simulation results like torques, forces, moment arms, etc. of each joint. The OpenSim's Application Program Interface (API) is written in *C++* and not only provides same features as the GUI, but also enables the user to make new analysis, add new features, and build new models. OpenSim uses SimBody, a high-performance, full-featured toolkit for internal coordinate multibody dynamic simulations that lend basic elements for simulations in OpenSim [60].

### 2.2.2  Inverse Dynamics

Inverse dynamics (ID) is the process of calculating forces and moments from measured kinematic information such as position, velocity, and acceleration. OpenSim needs kinematic information as well as necessary external reaction forces, and the model coordinates, to perform ID. Results of ID would be the kinetic information (forces and moments) which are necessary to keep the model in desired position and state. For a given posture, ID along with static optimization can be used in biomechanical simulations to predict which muscles should be activated and the net forces of those muscles. In robotics, moreover, ID can estimate the amount of torques that motors must generate to achieve a certain motion.
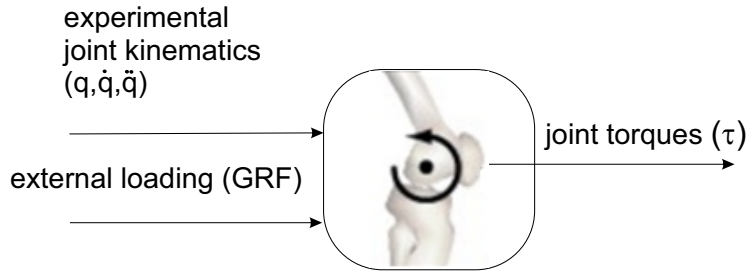


**Figure 2.4:** Data flow for inverse dynamics simulations in a joint torque driven model. Ground Reaction Force (GRF) and joint kinematics are used to calculate the joint torque. (Adapted from [17])

Figure 2.4 shows data flow of ID. Inputs to the system are the external loading (GRF) and the joint kinematics. The goal of ID is to calculate desired torques (or forces) to follow a predefined posture or motion trajectory. For example, given a certain posture to the lower extremity model in OpenSim, ID can determine necessary torques to allow model to hold a predefined posture or to follow a prescribed movement trajectory. The equations of motion for a musculoskeletal model are given as:

$$M(q)\ddot{q} + C(q,\dot{q}) + G(q) = \tau \tag{2.1}$$

where $q, \dot{q}$ and $\ddot{q} \in R^n$ are vectors of position, velocity, and acceleration. The DOF in the model are represented by $n$. $M, C$, and $G$ are the system mass matrix, the vector of coriolis and centrifugal forces, and

the vector of gravitational forces, respectively. The vector of torques ($\tau$) is the only term of the equation 2.1, which is unknown and can be computed from the known terms of the left hand side of the equation in ID. The kinematic information of the equation ($q, \dot{q}$ and $\ddot{q}$) can be obtained from inverse kinematics and motion capture techniques.

In this thesis, ID was used to determine a natural standing posture for the musculoskeletal model. A crouched posture provides better intrinsic stability compared to an upright one [63]. Therefore, we fixed the model's knee angle at 16 degrees of flexion, which is referred to as a mild crouch posture in [63]. The other joints coordinates in the model are then calculated using ID.

### 2.2.3 Optimization

Optimization can be used with ID to spread computed torques among muscles. Several global and local optimization algorithms including Interior Point, Covariance Matrix Adaptation (CMA), and Broyden-Fletcher-Goldfarb-Shanno (BFGS) have been implemented to be used in OpenSim. The objective function of the optimization problem can be defined in a variety of ways to be optimized subject to constraints of the problem. For instance, to spread torques gathered from ID among muscles, in order to keep the model in a predefined posture, one can minimize the sum of muscle forces (the objective function) subject to minimization of joint accelerations (constraining accelerations to zero).
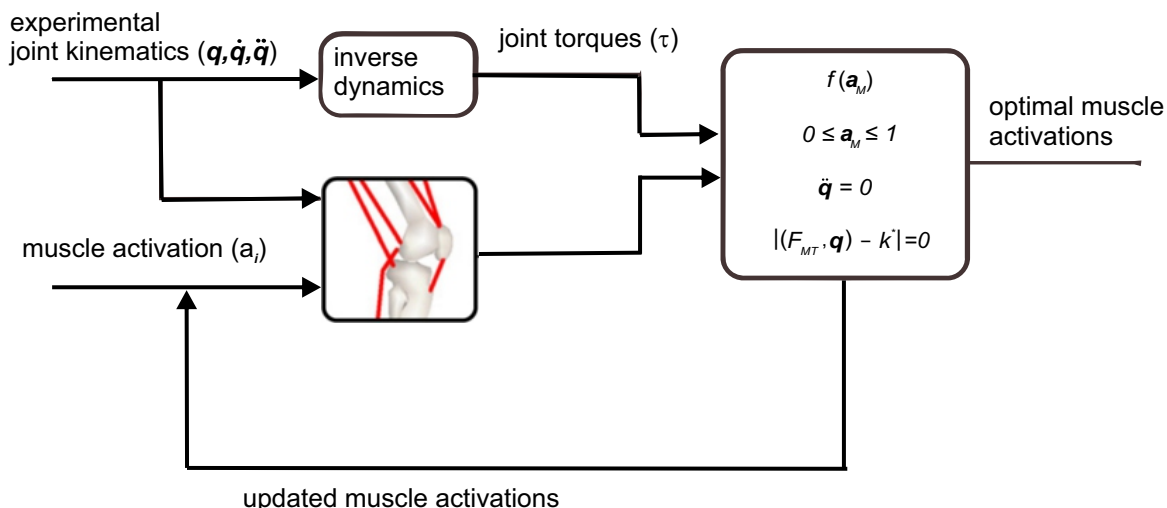


**Figure 2.5:** Static optimization with inverse dynamics. Joint kinematics are input to this system collected from experimental data. Muscle activations are parameters which should be optimized. A conventional starting point would be setting all muscle activations to maximum (1). $f(\boldsymbol{a}_M)$ is objective function. $\ddot{\boldsymbol{q}} = 0$ and $|k(\boldsymbol{F}_{MT}, \boldsymbol{q}) - k^* = 0|$ are constraints. (Adapted from [17])

Figure 2.5 shows data flow for static optimization with ID. Joint kinematics are collected from experiments. ID plays an important role in conversion of these kinematics to joint torques. Afterwards, the optimization was used to determine the minimum muscle activations to satisfy the problem criteria. Initial muscle activations can be set to any arbitrary number, but as a starting point for optimization, it plays an important role in

finding an optimal solution.

In this thesis, we used optimization for three different purposes. First, we developed a new formulation to constraint joint stiffness to a target stiffness in order to encourage co-activation of muscles (chapter 3). Second, it was used along with ID to determine a natural standing posture for the model. This model was used in chapter 4 for stiffness based optimizations of the knee and in chapter 5 for the stability test. Third, we used optimization to create different knee extension torques to verify the stiffness of the Short Range Stiffness (SRS) model (chapter 4).

### 2.2.4   Forward Dynamics

In opposition to ID, Forward Dynamics (FD) is designed to calculate kinematic information of the system from the applied torques and state of the system. In OpenSim, the state of the system is the set of joint angles, joint angular velocities, muscle fiber lengths, and muscle fiber shortening velocity. The skeleton is modeled as the set of rigid bodies; therefore, accelerations can be described in terms of inertia and applied forces as follows:

$$\ddot{q} = M(q)^{-1}[C(q, \dot{q}) + G(q) + F] \tag{2.2}$$

where $\ddot{q}$ is the vector of accelerations calculated as $M(q)^{-1}$ (inverse of the mass matrix) times the total applied forces and torques. Torques that are applied to the system are the sum of all joint torques ($\tau$) in addition to coriolis and centrifugal forces, ($C(q, q)$), gravitational forces($G(q)$), and other external applied forces ($F$). In OpenSim, the following inputs are required in order to apply FD to a model: actuators (for example: muscles), controls (activations of the muscles or other controls), and external forces (e.g., foot-to-ground contact model).

Figure 2.6 illustrates the data flow for an open loop controller based simulation. In this Figure ( 2.6), controllers adjust muscle forces based on the controller definition. Open loop simulation integrates the dynamics equation starting from initial state without feedback. After applying the muscle activations, forces of the muscles are computed and then coordinate accelerations are calculated and numerically integrated to compute the next state of the system in terms of positions and velocity of the coordinates. Integrating equation 2.2 would result in system coordinates velocity ($\dot{q}$) and positions ($q$). OpenSim provides a number of numerical integrators that the users can choose from depending on the problem.

For the posture perturbation simulations in this thesis, we used forward dynamics open loop simulations with a $5^{th}$-order Runge-Kutta-Feldberg integrator. The objective of these simulations is to identify the stability of different model configurations (level of the muscle co-activation and type of the muscle model).

### 2.2.5   Force Generators

To generate movement of rigid bodies and objects as well as to apply forces, OpenSim provides a collection of force elements. Springs are one of the actuators and force generators which could be employed in a point
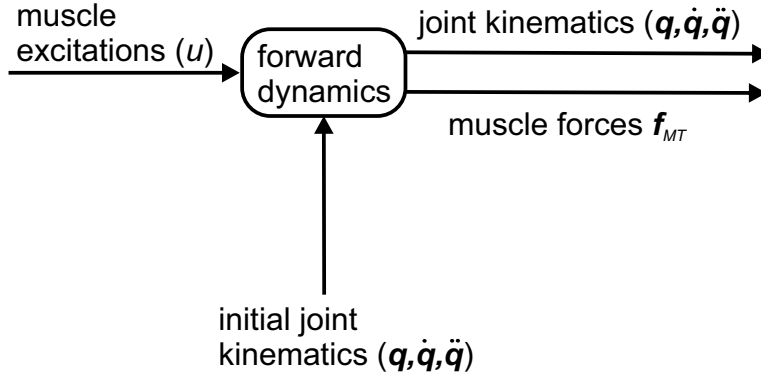
**Figure 2.6:** Forward dynamic simulation diagram. Inputs to the system are muscle excitation (calculated from muscle activation) and initial model kinematics ($q$, $\dot{q}$ and $\ddot{q}$). Numerical integration from equation of the system (Equation 2.2) would result in joint kinematics in a given time.

to point manner between two objects (*PointToPointSpring*), or it could be spread among several objects by routing through two or more points (*PathSpring*). Contact forces to provide support between the ground and the model or between peripheral objects and the model, are implemented in the OpenSim using a Hunt Crossley Force (HCF) model. Along with these elements for force generation there are other types of forces such as bushing forces and coordinate limit forces (which limits movement of coordinate between certain angles).

Figure 2.7 lists all of the different types of forces available in OpenSim. All of these forces are inherited from *Force* class and each has its own specifications. *Actuators_* is one of the force types in the OpenSim that can be derived and expanded. This is the base configuration for any type of actuators that are used in OpenSim. OpenSim provides different actuators such as *CoordinatActuators, PointActuators, PointToPointActuators, TorqueActuatores*, and *PathActuators*. Muscles are, in fact, a type of *PathActuator*.

Muscles are one of the most important force generators in the OpenSim. A muscle model is a component that transforms activation to force. Based on the complexity and accuracy of the muscle model, results can be compared with experimental studies. In OpenSim, a muscle model consist of a muscle in series with a tendon. Four types of muscles are provided as follows: Rigid tendon muscles (*RigidTendonMuscle*), Thelen model (textitThelen2003Muscle), and two Millard models, (*Millard2012AccelerationMuscle* and *Millard2012EquilibriumMuscle*). All of these models are a subclass of the *Muscle* class in OpenSim as shown in Figure 2.8.

*Millard2012EquilibriumMuscle* is a Hill-type muscle model in which the force of the muscle is calculated from addition of both active and passive force. In an equilibrium muscle model, the force generated by the
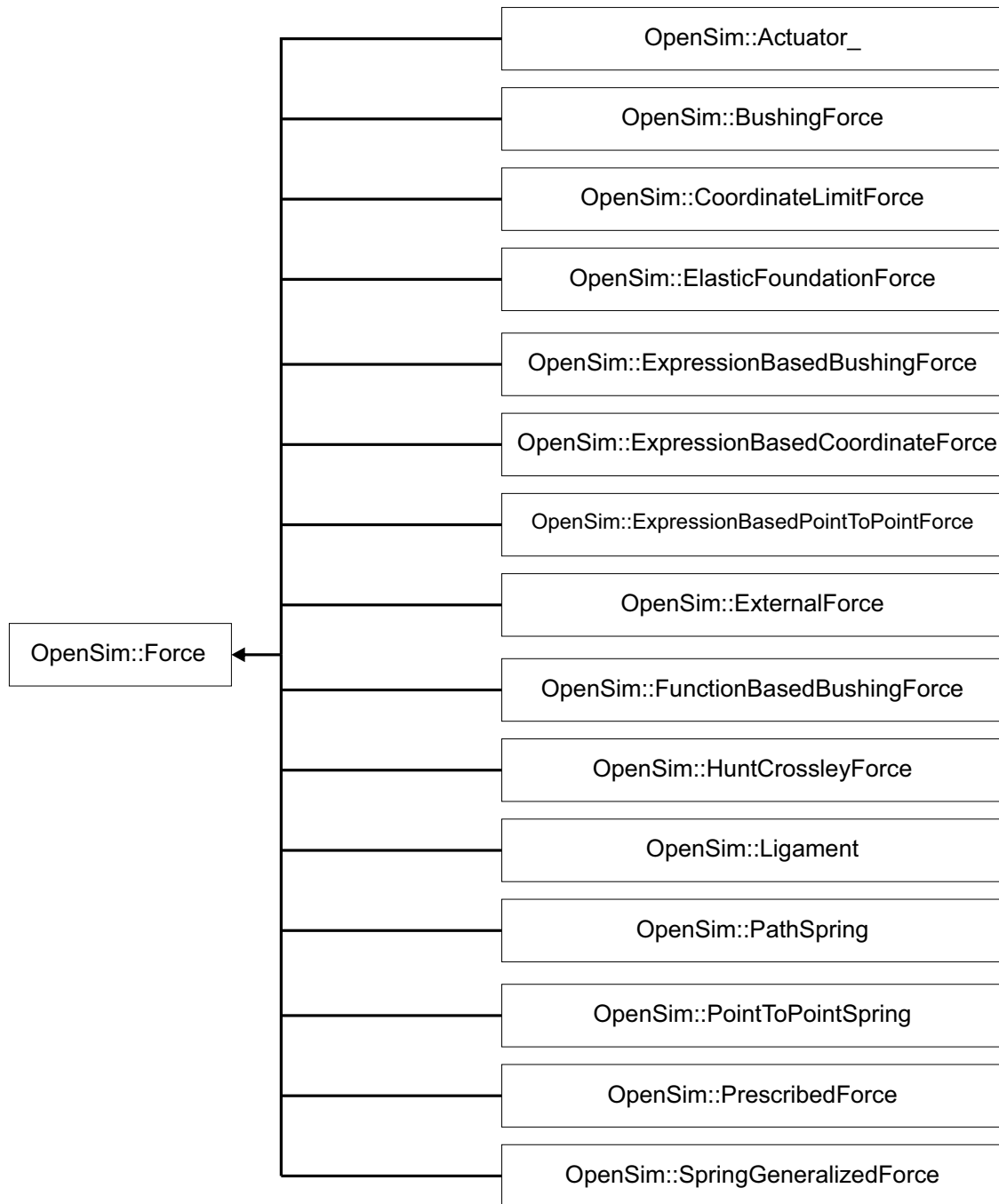
**Figure 2.7:** Class diagram of all force generators in OpenSim. *Actuators* is one of the classes. It is derived by several classes to form different types of actuators.
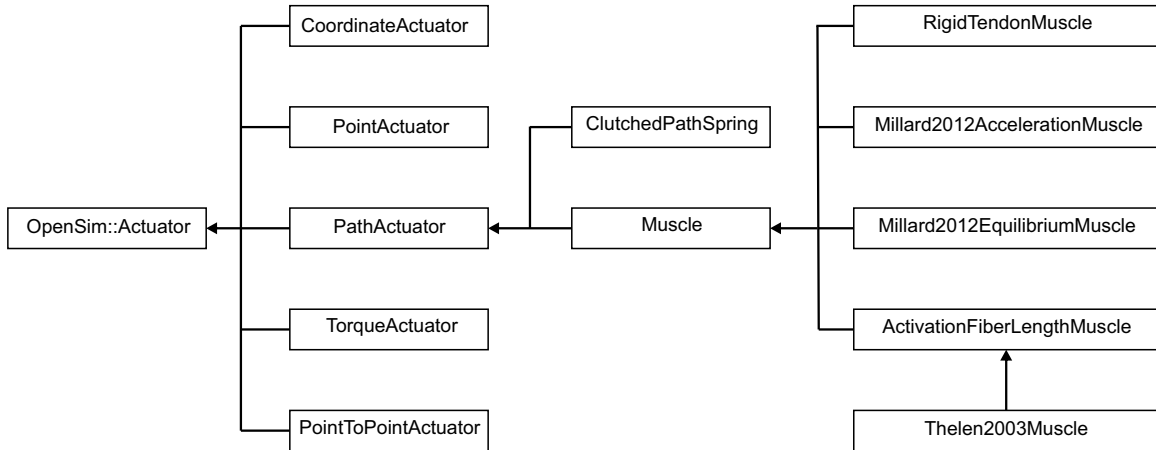
**Figure 2.8:** Actuators hierarchy in OpenSim. *Muscle* is a member of *PathActuator* class.

muscle fiber itself and the tendon is considered to be equal [39]. The active force of the muscle is calculated using an activation — a number between 0 and 1 — and is affected by the velocity and length of the muscle fiber.
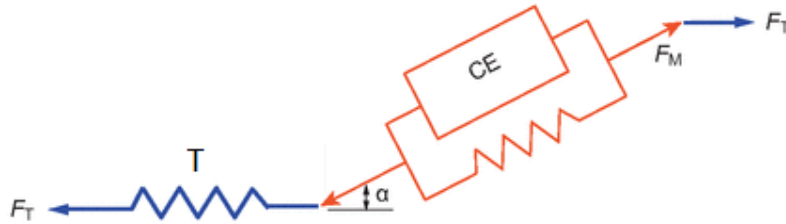


**Figure 2.9:** A muscle model consist of a contractile element (CE) arranged in parallel with an elastic element, representing muscle fibers. Both are in series with another elastic element representing tendon (T). $F_M$ and $F_T$ are muscle and tendon forces, respectively. $\alpha$ is pennation angle. Adapted from [47]

Figure 2.9 represents a Hill-type muscle diagram along with tendon. Figure 2.10 shows the active and passive parts of the force generated by a muscle as a function of its length. The peak for the active part of the force generated by the muscle fiber occurs at optimal length of the muscle and decreases when muscle becomes longer than its optimal length. However, the passive part starts generating force at lengths greater than the optimal fiber length.

## 2.3 Stability of Body

Postural stability is the ability to keep one's vertical Center of Mass (COM), with minimum sway, inside the Boundary of Support (BOS) defined by the area enclosed between one's feet. An amount of unavoidable sway due to small perturbation within the body or from external sources can happen without affecting balance
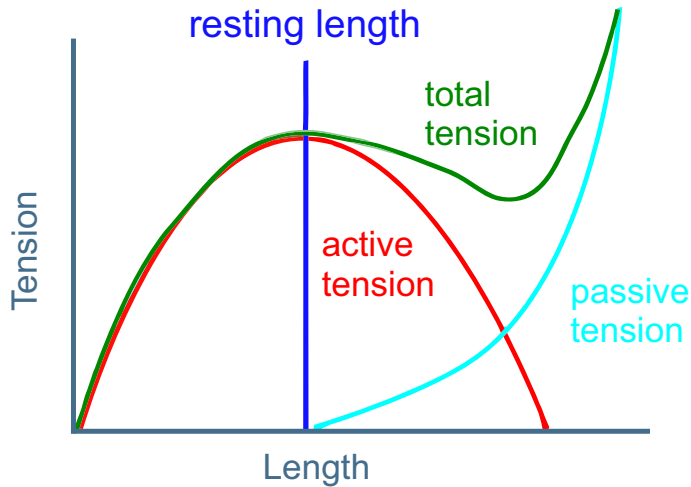
**Figure 2.10:** Active and passive tension of muscle fibers. These tensions are a function of length of the muscle fibers.

while for larger perturbations compensation is necessary. Balance control involves the body responding to external disturbances such as slippery surfaces, voluntary movements of the upper body, and external pushes. Since body motion can take place in all planes of motion, all coordinates are involved for posture stability and it is a difficult ability to recover.

To have a better understanding of postural stability, one should first have knowledge of factors that can affect it. Stability of the body should be preserved in order to stand or walk, and when an external perturbation disrupts the body's equilibrium, the body should be able to properly counter the perturbations. Postural stability of the body has two components to perform this task: natural (or intrinsic) stability of one's body, and the feedback responses that are engaged following a perturbation to react and maintain stability. Each component has its own effect on the stability and one of them can become more important compared to the other in different situations.

Responses to inputs from the sensory system are one strategy by which the body preserves its stability. However, responses from the nervous system are only one aspect of those strategies that the body uses to preserve its balance. Another aspect is the body's intrinsic mechanical stability. The body's built-in or intrinsic stability includes passive responses to perturbations that do not require active feedback control. The intrinsic stability of one's stance and gait pattern may partly compensate for diminished feedback responses to external stimuli and play an important role in the maintenance of balance. The greater the intrinsic stability, the less need for fast, and accurate reactive responses to control balance [27]. For this reason, the characterization of a patient's intrinsic stability may inform the assessment of fall risk in older adults. Nonetheless, such potential has yet to be studied. In order to unlock this potential, we must first understand

18

the degree to which different biomechanical factors affect intrinsic postural stability.

A number of biomechanical factors may contribute to the intrinsic stability of stance and help to compensate for diminished feedback responses. These include foot placement, postural configuration of the body, tonic muscle activity, intrinsic muscle properties, and behavioral factors (anticipation, attention, mood, fear) [63]. For example, foot placement can help to increase postural stability and prevent the body from swaying and falling. Furthermore, it has been suggested that foot placement direction and width had a significant effect on postural stability of construction workers working on stilts [48] . They found that standing with one's feet parallel to each other is more stable than placing one foot ahead of the other one and that a wider stance generally increased postural stability. Conversely, a recent simulation study found an unintuitive result that wider stance required more feedback response to maintain stability [2]. The intrinsic properties of muscles and tendons such as force-length and force-velocity properties also contribute to the stability of the body by instantaneously and passively responding to perturbations [4]. A recent study, using 3D musculoskeletal simulation, demonstrated that removing muscle intrinsic properties decreases the stability of a walking model under variety of perturbations [29]. Body posture is another factor that plays an important role in stability. For example, simulations have verified the intuitive notion that a crouched posture is intrinsically more stable than fully upright [63].

Muscle recruitment is another important factor in regulating intrinsic postural stability. Co-activation of antagonist muscles has been identified as the main mechanism to actively control joint stiffness in limb movements [25] and plays a role in many motor tasks [31, 13]. Naturally, co-activation of agonist and antagonist muscles happens in different tasks performed by muscles. In this regard, muscle co-activation is necessary for stabilization of shoulder, elbow, wrist, and finger [69]. Co-activation can also result in stiffer joint and could lead to more stability. Hence, increasing co-activation of the agonist and antagonist muscles at hip, knee, and/or ankle may result in higher stability. Measuring postural stability is commonly done by analyzing the body's center of mass projected to the ground (COM) relative to the body's boundary of support (BOS), which is the area of the ground enclosed by the feet. A person (or model) is considered to be stable if their COM lies within the BOS. For our simulations, the model's posture was configured in such a way that the COM was initially aligned to the centroid of the BOS (Figure 2.1). During posture perturbation simulations, the time from the end of the perturbation to the time at which the COM leaves the BOS was measured as the time-to-fall. The time-to-fall was then converted to a stability index as a metric of overall postural stability of the model, the details of which are explained in chapter 5.

# CHAPTER 3

# STATIC OPTIMIZATION

Optimization is the process of selecting the best possible solution for a specific problem with well-defined objectives under well-defined conditions (constraints). The optimization algorithms fall into two categories: global and local algorithms. A parametric function known as objective function, loss function, or cost function (usually in minimization), is the optimization problem, in which parameters have to be optimized (usually minimized or maximized) subject to a set of equality and/or inequality constraints. Optimization is a common method to solve system identification problems in biomechanical studies. In this chapter we explore how optimization can be used to calculate a set of muscle forces or activations in order to perform a task in a musculoskeletal model and develop a new optimization formulation that can improve the accuracy of such simulations.

## 3.1 Introduction

### 3.1.1 Static Optimization

Optimization is used to solve a number of different problems in biomechanical simulations. For instance, optimization can be used along with Inverse Dynamics (ID) to spread net joint torques into individual muscle forces. Static optimization is a common approach to select muscle activations or muscle forces that are required to achieve desired joint torques. The "static" qualifier in the term static optimization refers to the fact that this problem is solved at only one instance in time. Such problems are typically redundant: multiple combinations of muscle forces can result in the same net joint torque; therefore, we need some criteria to select a particular, desirable set of muscle forces from all possible combinations. The objective is usually to minimize the energy necessary to perform the biomechanical task [17]. For a static equilibrium task, such as standing, minimizing the sum of squared muscle activations, while constraining joint accelerations to zero, is a standard way to distribute forces among muscles to stabilize a model [11, 30].

In OpenSim, an optimization solver algorithm would be chosen based on the type of problem. For an unconstrained problem with unbounded coordinates, OpenSim will use Limited-memory Broyden-Fletcher-Goldfarb-Shanno algorithm (LBFGS) [34], while for problems with constraints to satisfy, the Interior Point (IPOPT) algorithm would be used to enforce the constraints [66]. Furthermore, users can provide their own algorithm to solve an optimization problem in OpenSim. Since our problem had constraints, we used Interior

Point algorithm to solve the problem.

In an optimizations related to a biomechanical task of a musculoskeletal model, the objective function, to some extend, minimizes the required forces or torques. Usually, desired joint torques are calculated from ID. When joint torques are calculated, optimization is a reliable way to distribute torques among muscles. The objective functions, such as minimization of energy costs to perform the task, minimization of muscle stress, or sum of squared muscle forces or muscle activation, commonly are opted to solve the problem. One common approach, to perform static optimization in OpenSim, is to minimize the sum of squared muscle activations [11, 30]. Using this function, as an objective, provides straightforward analytical equation for its gradient that can be used in optimization to reduce the problem solving time.

### 3.1.2   Co-activation of Muscles in Static Optimization

Muscle co-activation happens in a situation where the agonist and antagonist muscles activate together to support and stabilize the corresponding joint. For example, to stiffen the elbow, biceps and triceps muscles can be activated simultaneously (co-activated). Traditional static optimization results in limited muscle co-activation because the optimization's objective function minimizes forces or activations of antagonist muscles. The co-activation of agonist and antagonist muscles has a profound effect on stabilizing body movements and is involved in a variety of daily activities [1, 62]. Higher co-activation can take place when a person is walking on a slippery surface, and even when the person expects a slippery surface [6]. Besides, the activation of agonist and antagonist muscles progressively increases with age. Current studies suggest that older adults have more co-activation in the electromyography (EMG) signal gathered from their muscles [36, 38, 40]. Therefore understanding the effects of muscle co-activation on postural stability may be important for understanding balance in older adults.

It is widely believed that the co-activation of agonist and antagonist muscles, increase joint stability and reduce joint laxity in higher limb velocity [23, 22]. Furthermore, high co-activation might increase stiffness of the joints and provide more control over body stability. Therefore, higher co-activation might be a strategy by which body elevates its stability during standing or gait [36, 38]. Some other studies, on the other hand, suggest that higher amount of co-activation is a consequence of aging, which subsequently results in lower control over the stability by reducing the movability of joints [40].

Hence, a new method is necessary to evoke the co-activation in simulations and to allow the muscles to pick their activations. There have been few studies to support co-activation while optimizing muscle forces. Previous methods have required direct manual specification of co-activation levels, or have separated agonist and antagonist muscle groups and run two optimizations to spread forces among muscles of each group [52]. To overcome these limitations we have developed a new technique to allow optimization of posture forces without prescribing co-activation and without separating muscles.

## 3.2 Methods

### 3.2.1 Standard Static Optimization Formulation

Static optimization is a common approach to select muscle activations and forces that achieve a desired set of joint torques. For a static equilibrium task, such as standing, a standard static optimization approach is to minimize the sum of squared muscle activations subject to constraining joint accelerations to zero (so that the model remains stationary). The objective function is formulated as follows:

$$f = \sum_{i=1}^{n} a_i^2 \tag{3.1}$$

where $a_i$ is the activation (between 0 and 1) of the muscle number $i$ and $n$ is the number of muscles in the model. The optimization is performed subject to the following constraint:

$$C_1 = \ddot{\boldsymbol{q}} = 0 \tag{3.2}$$

where, $\ddot{\boldsymbol{q}}$ is a vector of acceleration of all the coordinates in the model. However, minimizing overall muscle activation will result in limited muscle co-activation. Hence, a new constraint, in optimization formulation, is needed to encourage the co-activation.

### 3.2.2 New Constraints to Encourage Co-activation

In order to achieve a static optimization result that includes co-activation, a new objective function was formulated. Instead of prescribing co-activation levels directly between agonist and antagonist groups, it was desired to let co-activation happen while still minimizing the forces and letting the optimizer freely spread forces among muscles. We chose joint stiffness as a constraint in optimization formulation as a potentially valuable approach to encourage the agonist and antagonist muscle activations. To this end, we formulated an additional constraint term to the optimization problem that included a target joint stiffness. The additional constraint was formulated as follows:

$$C_2 = k_a - k^* = 0 \tag{3.3}$$

where $k_a$ is the measured stiffness of the joint and $k^*$ is the target stiffness (desired stiffness of the target joint). This new formulation was used to encourage co-activation while the activation of the muscles were minimized. By using joint stiffness as an intermediate variable to encourage co-activation, it was possible to achieve muscle co-activation at different levels while satisfying all constraints in the problem. The level of co-activation in muscles can be controlled by the target stiffness which was defined in the optimizer.

### 3.2.3 Numerical Approach to Measure Joint Stiffness

Since our static optimization approach now includes a term for joint stiffness we needed a method to measure the actual joint stiffness, $(k_a)$, directly from the model, after applying muscle activations. OpenSim does not provide joint stiffness as an output, but it is possible to measure joint torques and angles from the model. Hence, joint stiffness was measured using finite differences. Joint stiffness is defined as:

$$k_a = \frac{\Delta \tau}{\Delta q} \qquad (3.4)$$

where $\tau$ denotes the target joint torque and $q$ is the target joint coordinate. To measure stiffness, the joint was perturbed by the amount $\Delta q = 1 \times 10^{-6}$ rad. The joint torque was measured before and after perturbation. $\tau$ and $q$ were measured directly using the OpenSim built-in properties; the ratio of change in torque to change in coordinate resulted in stiffness of the joint.

### 3.2.4 Analytical Approach to Measure Joint Stiffness

An alternative approach could be taken to measure the joint stiffness. This approach was obtained by expanding Equation 3.4 to eliminate the need for numerical perturbation of the coordinate. Hence, it is computationally more efficient in comparison to the numerical approach, and would increase the optimization speed.

$$k_a = \frac{\partial \boldsymbol{r}^T}{\partial q} \boldsymbol{F} + \boldsymbol{r}^T \boldsymbol{K}_D \boldsymbol{r} \qquad (3.5)$$

Equation 3.5 was used to map the stiffness of the system to the joint stiffness [37]. $\boldsymbol{F}$ is the vector of forces acting on the target joint in the system and $\boldsymbol{r}$ is the vector of moment arms of those forces. We used OpenSim's *MomentArmSolver* to compute the moment arms and moment arm derivatives. $\boldsymbol{K}_D = diag(\boldsymbol{K})$ is diagonal matrix of $\boldsymbol{K}$, and $\boldsymbol{K}$ is the vector of stiffness of acting forces.

## 3.3 Evaluations

### 3.3.1 Verification of Numerical Approach to Measure Stiffness

The analytical approach (Equation 3.5) is derived from the definition of the stiffness. Hence, it can be used to certify the new method for measuring the joint stiffness (numerical approach). To this end, two test models were developed: 1) rotational spring at the joint, and 2) muscle-like springs connected to the body. For the first one, model implemented with one rigid body connected to ground with a single joint and one Degree of Freedom (DOF). A bushing force (with 3 rotational and 3 translational stiffnesses) was added at joint (Figure 3.1a). To verify, all the stiffnesses were set to zero except one rotational stiffness at the direction of joint's rotation ($Z$ direction). We explicitly set the stiffness in the bushing force and then compared this

value to the measured joint stiffness using the numerical perturbation method (Equation 3.4). We examined the stiffness for a set of different stiffness configurations from -10 to 10 Nm/rad (with the step of 1 Nm/rad)
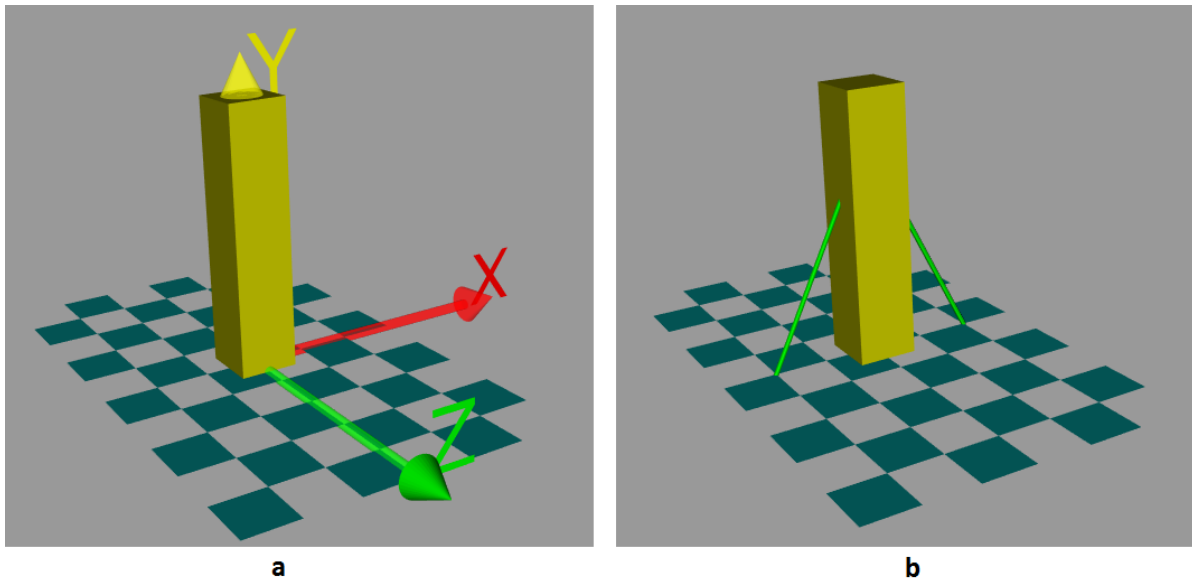


**Figure 3.1:** Model for testing stiffness measurement method with one rigid body (yellow block), a 1 DOF joint (located at the origin of the coordinate frame) and a bushing force at the joint (a) or 2 springs (green lines) (b). The models were used to test the numerical perturbation and analytical methods for measuring the joint stiffness.

A second model with two springs was used to evaluate the analytical equation for joint stiffness. To this end, we removed the bushing force from the joint and added two symmetric springs to the model (Figure 3.1b). To test this model, lengths of the springs were both fixed and did not change during the test. Then we increased stiffness of both springs from 0 to 1000 Nm (with the step of 100 Nm). The measured stiffness using numerical method was compared to the stiffness that calculated using the analytical method (equation 3.5) and reported in the result section.

### 3.3.2   Evaluation of New Static Optimization

A simplified upper arm model with a one DOF elbow joint was used to test new formulation (Figure 3.2). The shoulder was locked to have a simple model with just one coordinate (the elbow angle). Muscles in this model include the Short Head Biceps Brachii (Biceps-Short), Long Head Biceps Brachii (Biceps-Long), Brachioradialis (BRA), Long Head Triceps Brachii (TRI-Long), Lateral Head Triceps Brachii (TRI-Lat), and Medial Head Triceps Brachii (TRI-Med) (see Appendix B). Target stiffness at elbow was varied from 0.5 to 8 Nm/rad. For each target stiffness, the optimization was run in order to find the minimum set of activations to achieve target stiffness and zero acceleration at the elbow.
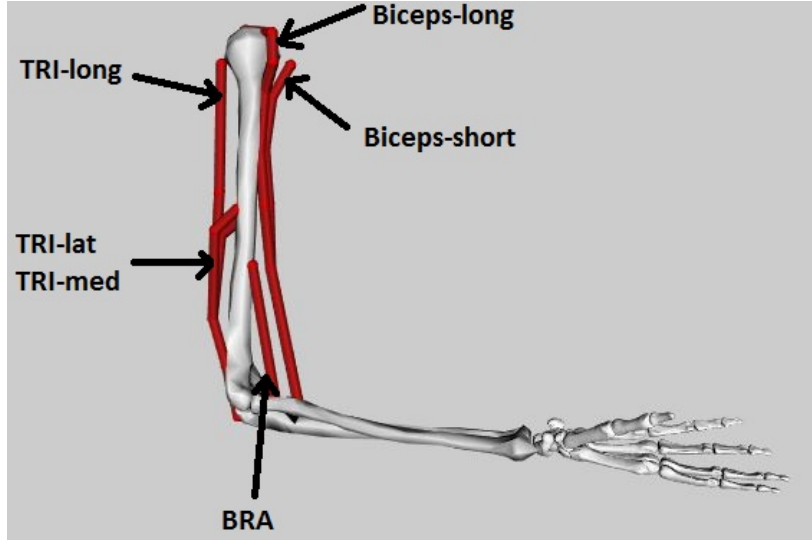
**Figure 3.2:** Arm model with 1 DOF at elbow and 6 supporting muscles: Short Head Biceps Brachii (Biceps-Short), Long Head Biceps Brachii (Biceps-Long), Brachioradialis (BRA), Long Head Triceps Brachii (TRI-Long), Lateral Head Triceps Brachii (TRI-Lat), and Medial Head Triceps Brachii (TRI-Med)

## 3.4 Results

### 3.4.1 Joint Stiffness Measurement

Our result regarding the measurement of the joint stiffness (Figure 3.3 and Figure 3.4) supports the accuracy of the numerical method described in section 3.2.3. Figure 3.3 shows the target stiffness versus measured stiffness using numerical approach for the model with bushing force (Figure 3.1 a). For this model, the Mean Square Error (MSE) for measured stiffness and target stiffness is $3.84 \times 10^{-18} (Nm/rad)^2$ when $dq = 1 \times 10^{-6} rad$ was chosen.

For the model with two springs (Figure 3.1 b), measured stiffness using numerical approach is the same as the stiffness computed using analytical approach (described in section 3.2.4) at the joint. The MSE for measured and analytical stiffness for this model was $4.99 \times 10^{-8} (Nm/rad)^2$ when $dq = 1 \times 10^{-6} rad$ is chosen. Figure 3.4 shows results of these measurements. Overall our findings indicate that the perturbation method is a reliable mean to measure joint stiffness.

### 3.4.2 Static Optimization with Target Joint Stiffness

The result of our new static optimization with the arm model for the range of 0.5 to $8Nm/rad$ target elbow stiffnesses shows an increase in combined activation of agonist and antagonist muscles (Figure 3.5).

Some muscles, such as Biceps-Long, and TRI-Long, were not significantly affected when the elbow stiffness increased. Other muscles, in both groups, such as Biceps-Short and TRI-Med provided more force and had more effect on the elbow stiffness. Figure 3.5, also demonstrates that some muscles reached their maximum
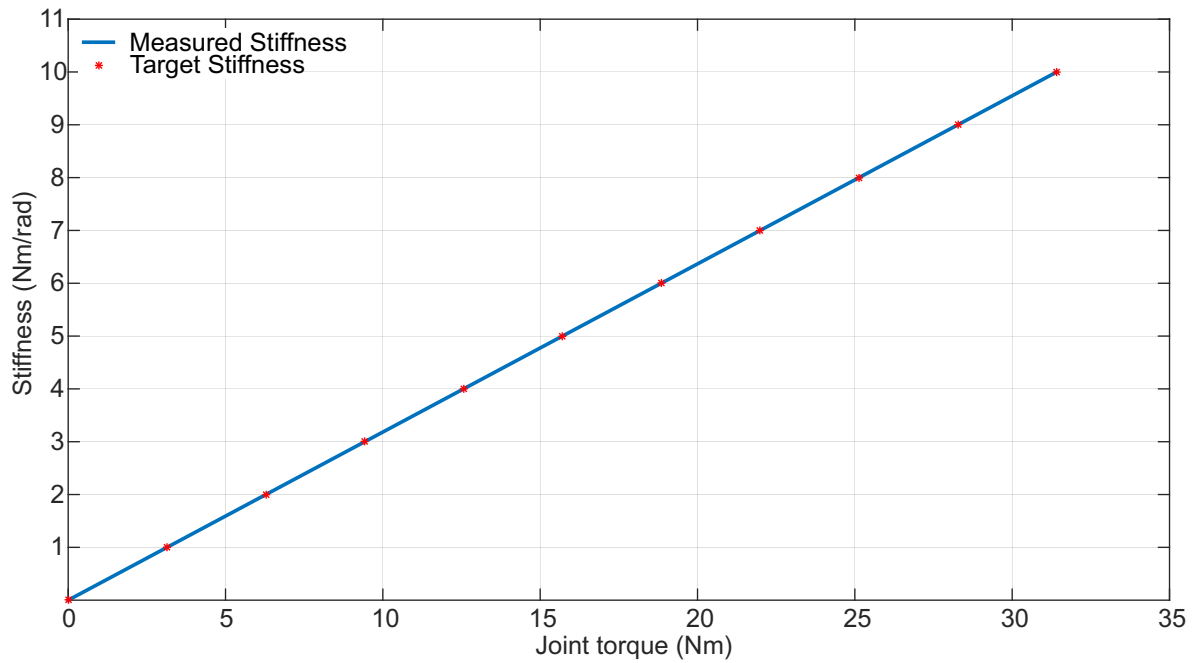
**Figure 3.3:** Measured (solid line) and target stiffness (strike) of model with bushing force against the joint torque.
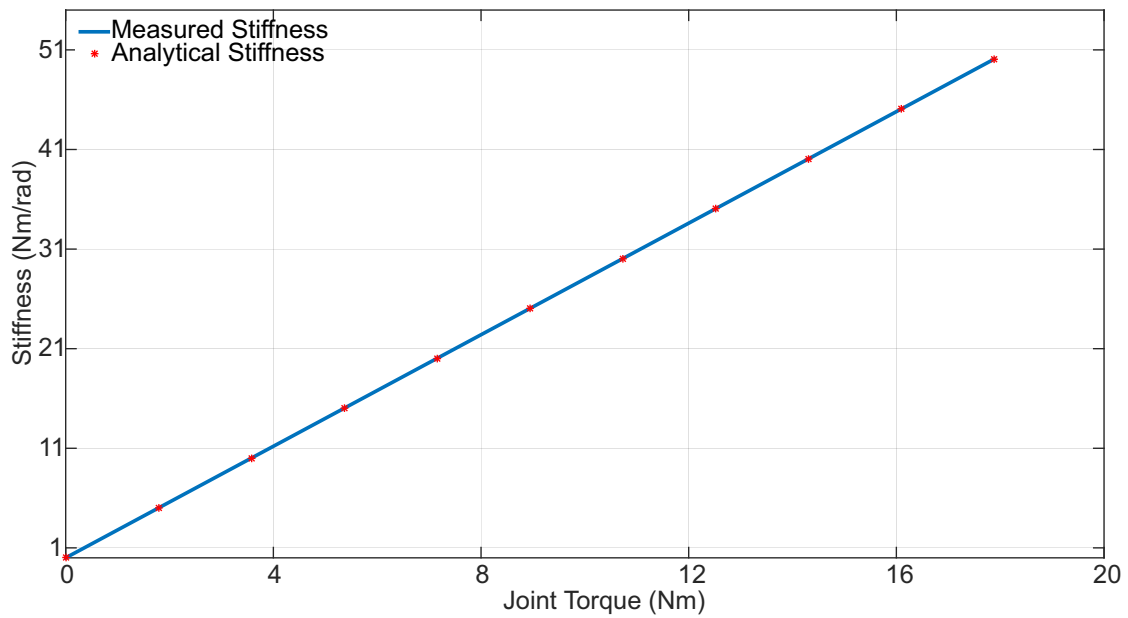


**Figure 3.4:** Measured (solid line) and target stiffness (strike) of the model with two springs against the joint torque.
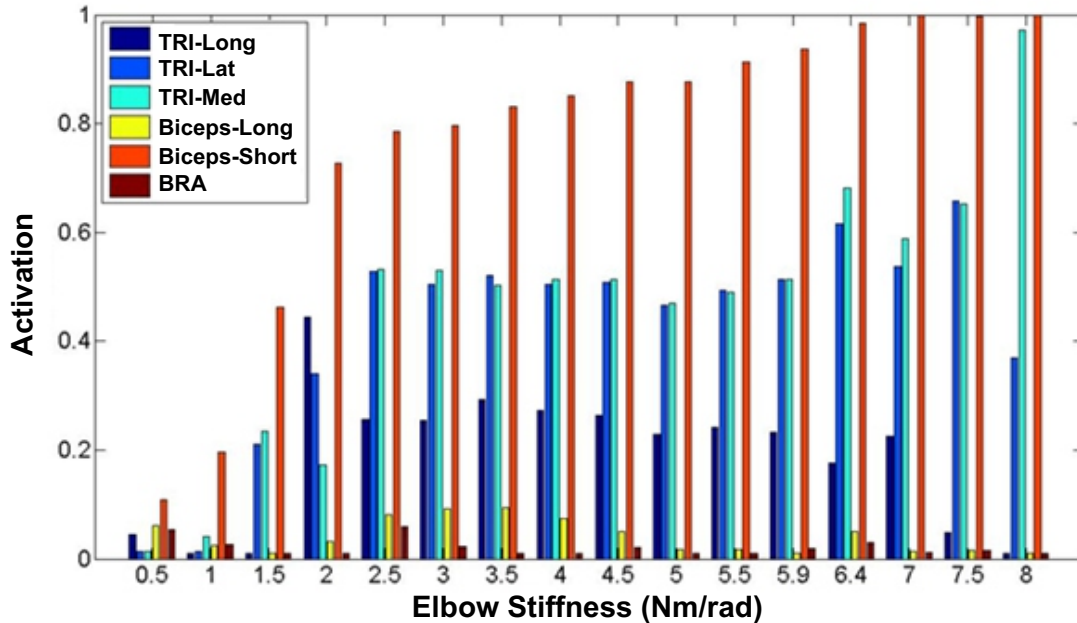
**Figure 3.5:** Six muscle activations in both groups of elbow flexors and extensors. Forcing the elbow stiffness to increase results in higher activation in both groups of muscles, which in fact represents the co-activation of muscles.

activation at the target stiffness of $8Nm/rad$: Biceps-Short is maxed out, and TRI-Med is close to be fully activated.

## 3.5 Discussion

### 3.5.1 Joint Stiffness Measurement

Although OpenSim is a powerful biomechanical simulation toolkit that offers a variety of analysis techniques, there are many metrics that OpenSim does not provide as a built-in feature. Stiffness of the joint is one such a metric for which there is no built-in measurement method. However, it is possible to extend the API to measure these new parameters. In this thesis, we implemented two methods to measure the joint stiffness. A numerical method as well as an analytical method was implemented and verified. Our finding demonstrates that both methods are accurate and could be used in different situations. Based on the problem, either of these methods could be more efficient than the other one. For a model with fixed posture (and constant moment arms) the analytical approach could be better solution, because moment arms and moment arm derivatives can be computed one time and used. The numerical approach, on the other hand, is better suited for situations when the posture and, consequently, the moment arms are constantly changing, such as for dynamic movements like walking.

### 3.5.2 Underestimated stiffness Range

The arm model optimization showed that increasing the stiffness of the elbow, successfully resulted in a higher co-activation in agonist and antagonist muscles. In this model, six muscles are provided to support the elbow movement. Biceps-Short, TRI-Long, TRI-Lat, TRI-Med muscles provide more forces while the Biceps-Long, and BRA are less affected. Setting target stiffness to 8 Nm/rad, Biceps-Short is in its maximum activation and TRI-Med is close to its maximum activation, which would suggest that it might not be feasible to increase elbow stiffness to higher levels, for the arm model. This level of stiffness is considerably lower than those have been measured in experimental studies [5, 51]. [51] reported that elbow stiffness is between 0 and 150 Nm/rad for elbow flexion torques ranging from 0 to 20 Nm. We expect that the highly underestimated elbow stiffness is due to the muscle model which was employed, the Hill-type muscle model [39].

The stiffness of the Hill-type muscle model is known to be lower than experimental measurements, because it does not capture the intrinsic stiffness of the muscle tissue [67]. It is suggested that endpoint elbow stiffness can be estimated from the Short Range Stiffness (SRS) of a muscle [28]. The stiffness of their model closely matched experimental measurements reported by previous studies [5, 51]. Also, SRS model is integrated into the knee muscles and provided a model to estimate the knee stiffness verified with experimental data for the knee stiffness [52]. We believe the measured elbow stiffness using the perturbation method, which was used to satisfy the stiffness constraint in the optimization, is highly diminished because of the Hill-type muscle model. It would be beneficial to integrate the SRS model to OpenSim and use that in the optimization, which is described in the following chapter.

### 3.5.3 Co-activation with Lower Extremity Model

In this chapter, we used the arm model as a toy model to test the novel optimization formulation. However, employing a more complex model with more DOFs and several muscle groups seems to be necessary. Hence, we opted to use the lower extremity model (Figure 2.1). Our work would benefit from using this model in many ways. First, after optimizing the model and co-activating the muscles, we will be able to run posture simulation and examine the effect of co-activation on the stance stability. To date, a muscle model with the intrinsic SRS has not been used in forward simulations. In chapter 5, we will describe our method for the postural stability test.

Second, there are several bi-articular muscles in most joints of the human body. Increasing the stiffness of a single joint might have an effect on the other joints mainly due to bi-articular muscles. Analyzing our optimization technique with a more complex model would provide sufficient evidence for such a case. In Chapter 4, we will employ the lower extremity model by targeting the knee stiffness. Optimizing the knee stiffness in the lower extremity model would enable us to study the effect of higher knee stiffness due to the co-activation of muscles on the other joints. For instance, the Medial Gastrocnemius muscle is a bi-articular muscle between the knee and the ankle. Also, the Rectus Femoris muscle is coupled to the knee and the hip.

Therefore, this muscle will be affected by the knee stiffness. Tracking other joints' stiffnesses and muscle activation will provide us the ability to investigate the effect of co-activation of knee muscles on the other joints (the hip and the ankle).

# Chapter 4

# Short Range Stiffness

Chapter 3 described the existence, and benefits of co-activation patterns of muscles in biomechanical tasks that the human body performs, but previous formulations of optimization ignored muscle co-activation. As discussed in chapter 3, joint stiffness can be used as an intermediate variable to encourage co-activation. However, the Hill-type muscle model, which was employed in the model, was a restriction. This is an issue because the stiffness of the joints is dominated by the stiffness of muscles and mainly by intrinsic muscle stiffness, the so called Short Range Stiffness (SRS).

This chapter describes implementation of a muscle model that captures the intrinsic stiffness of the muscle, as well as how this model could be integrated into the new optimization formulation. This muscle model will be used in our simulations of postural stability in chapter 5. We will refer to this muscle model as the *SRSMuscle*. Employing the *SRSMuscle* model could be a huge improvement to the overall stability of the model, but has its limitations. These limitations will be discussed in detail in the discussion section (section 4.5).

## 4.1   Introduction

Stiffness of the Hill-type muscle model is known to be less than the stiffness of muscle in the human body. While some passive structures, like ligaments, contribute to joint stiffness, the stiffness in the direction that joints move is due primarily to muscle-induced stiffness. Moreover, during static equilibrium, muscle stiffness is dominated by the short range stiffness of muscle tissue [52, 28]. SRS is the initial response of the muscle to sudden change, and mainly lasts for a small amount of change in muscle fiber length [54]. Since an accurate model is required to capture the intrinsic stiffness, it is necessary to implement the *SRSMuscle* model in OpenSim.

This chapter describes the following methods that have been used. First, we will present our implementation of the *SRSMuscle* model in OpenSim. Stiffness of this muscle model was verified, and it will be used in chapter 5 in forward simulations. Second, we will describe the implementation of the SRS estimation in our optimization to satisfy the stiffness constraint (Equation 3.3). In this way, optimization can be used with a model that uses the Hill-type muscle model, while at the same time benefiting from SRS modeling to estimate the joint stiffness. An analytical approach is used to map muscle stiffness to joint stiffness.

## 4.2 Methods

### 4.2.1 *SRSMuscle Model*

The *SRSMuscle* class was implemented by extending the *PathSpring* actuator in OpenSim. *SRSMuscle* class needs to redefine two methods. First, the new class should define a new method for stiffness assignment. Recently, a theoretical model of SRS has been proposed, whereby a muscle fiber's stiffness, $k_M$ is proportional to the active muscle force and the inverse of the optimal fiber length ( [12]):

$$k_M = \frac{\gamma f_M}{l_M^\circ} \tag{4.1}$$

where $f_M$ is the active muscle fiber force and $l_M^\circ$ is optimal length of the muscle fiber and $\gamma$ is a constant equal to 23.4 [12]. The value of $f_m$ and $l_M^\circ$ are extracted from the Hill-type muscle model. Equation 4.1 was used to calculate stiffness for *SRSMuscle*.

Second, we need to have a new method in order to set the force of the *SRSMuscle*. To do so, muscle length can be initialized in a way to produce the force intended. Equation 4.2 describes this length calculation.

$$l_o = l - \frac{f}{k_M} \tag{4.2}$$

When the force of *SRSMuscle* is known, the actuator resting length ($l_o$) can be calculated using the Equation 4.2. The length ($l$) depends on posture of the model.

### 4.2.2 SRS Implementation in Optimization

Equation 4.1 describes the SRS of a muscle. The overall stiffness of a musculotendon unit, $k_{MT}$ can be estimated as the stiffness of the muscle fiber and the stiffness of the tendon in series (see Figure 2.9):

$$k_{MT} = \frac{k_M k_T}{k_M + k_T} \tag{4.3}$$

where $k_M$ is the muscle stiffness calculated using equation 4.1 and $k_T$ is the tendon stiffness. We used the tendon stiffness provided in the Hill-type muscles of the OpenSim model which is adopted from Zajac (1989). The joint stiffness can be estimated by accounting for all musculotendon units crossing the joint:

$$\boldsymbol{K}_{MT} = \begin{bmatrix} k_{MT1} & 0 & \dots & 0 \\ 0 & k_{MT2} & \dots & 0 \\ \vdots & \vdots & \ddots & 0 \\ 0 & 0 & 0 & k_{MTn} \end{bmatrix} \tag{4.4}$$

$$k_a = \frac{\partial \boldsymbol{r}^T}{\partial \boldsymbol{q}} \boldsymbol{F}_{MT} + \boldsymbol{r}^T \boldsymbol{K}_{MT} \boldsymbol{r} \tag{4.5}$$

where $k_{MTi}$ is the musculotendinous stiffness of the $i^{th}$ muscle, $k_a$ is the joint stiffness, $\boldsymbol{r}$ is the vector of moment arms of the muscles, $\boldsymbol{F}_{MT}$ is the vector of musculotendinous forces, and $n$ is the number of muscles in the model.

## 4.3  Evaluation

### 4.3.1  Evaluation of the Stiffness of *SRSMuscle* Model

The *SRSMuscle* is designed to address the issue of underestimated stiffness in the Hill-type muscle model. Hence, the *SRSMuscle* was validated by measuring the knee stiffness in our lower extremity model at different levels of applied knee extension torques, using the analytical method, and comparing it to experimental measurements reported by [52]. We performed standard static-optimization (minimizing the sum of squared muscle activations) with a target knee flexion torque excluding gravity in the range of -40 to 60 Nm, according to the [52] protocol. Since the data for this experiment does not include co-activation, we excluded antagonist muscles for both flexion and extension phase. To match the experimental setup of a participant sitting in an reclined posture with a bent knee, the knee angle in our model was set to 60 degrees and back resting angle was set to 15 degrees. The hip extension angle was also set to 90 degrees to match the protocol proposed in [52]. Additionally, We measured active knee stiffness ($k_a$) by only using active fiber forces. Then, we verified the stiffness of our model by comparing it to experimental data.

### 4.3.2  Evaluation of the SRS Static Optimization with Lower Extremity Model

We performed optimization for target stiffnesses in the knee from 150 to 900 Nm/rad with 50 Nm/rad step using the model with the Hill-type muscles and with the formulation described in sections 3.2.1 and 4.2.2. We measured muscle forces and activations for different levels of target knee stiffness. We also compared the actual stiffness of the knee joint — measured by the analytical method — in SRS model to our target stiffness.

## 4.4  Results

### 4.4.1  *SRSMuscle* Model Evaluation Results

Figure 4.1 shows the measured stiffness of the knee in the model with the Hill-type muscles in blue, model with *SRSMuscle* in red and experimental data collected from the [52] in green. As can be seen, the Hill-type muscle model does not provide sufficient stiffness. So, the stiffness of model which uses this muscle model is low compared to the experimental results. However, the *SRSMuscle* model has improved stiffness, the amount of stiffness has error compared to the experimental data. Mean Percentage Error (MPE) for extension phase is 6.26% and MPE is 9.89% for flexion phase verification. Stiffness of the mode with Hill-type muscle was

measured for extension phase (positive torques) of the verification and MPE for this model is 90.5%. MPE for felxion phase was 66.92%.
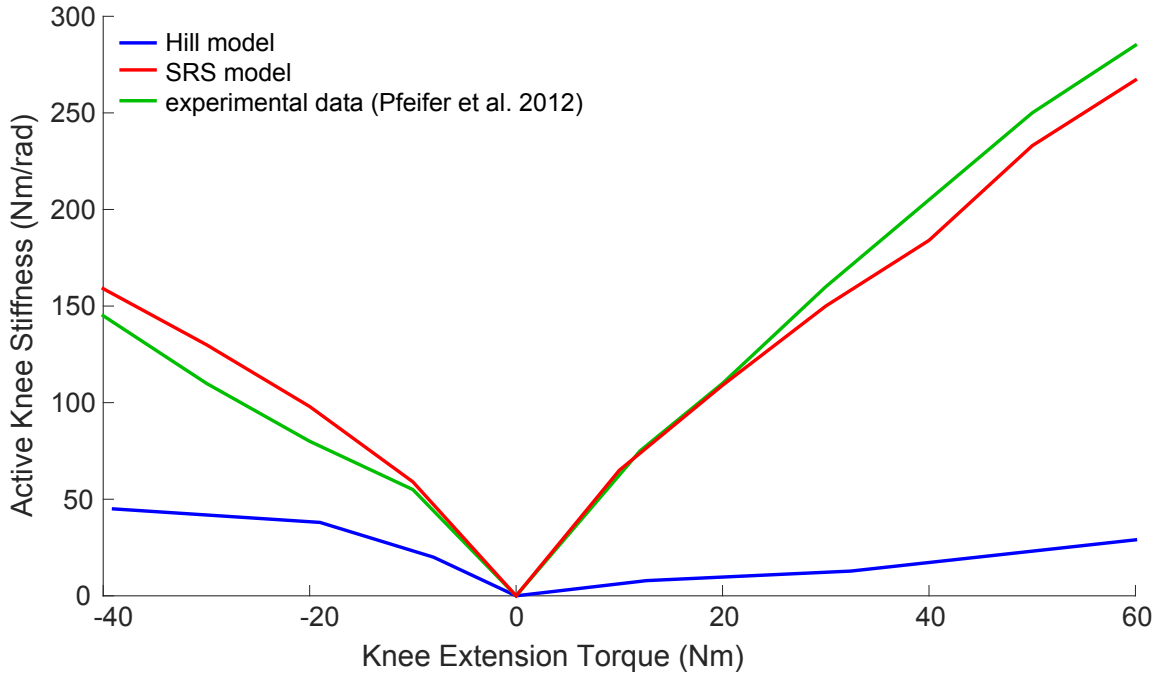


**Figure 4.1:** Active knee joint stiffness versus applied knee flexion/extension torque for models of Hill-type muscle (Hill; blue), Short-Range- Stiffness muscle (SRS; red), and experimental results ( [52] green)

### 4.4.2   SRS Static Optimization Evaluation Results

Figure 4.2 shows the activation of nine selected muscles for all different levels of target stiffness. We opted to show result of these muscles because these muscles are activated more than 10% at the highest stiffness level. Our static optimization results exhibited broad recruitment of lower extremity muscles to achieve additional knee stiffness. In total we tested 16 levels of target knee stiffness, and at each step activation increased between agonist and antagonist muscles of knee as well as muscles that span the ankle and hip. Interestingly, the per-step increase in muscle activation was not uniform across lower extremity muscles or within each muscle: certain steps in target stiffness resulted in larger steps in activation than others, and some muscles decreased in activation as stiffness increased.

To illustrate the co-activation of antagonist muscles, we grouped muscles corresponding to knee, hip, and ankle flexion/extension, and plotted the average muscle forces in each group for all levels of target stiffness. Figure 4.3 shows the results of average muscle forces for these groups. The groups are the hip flexors, hip extensors, knee flexors, knee extensors, ankle dorsi-flexors, and ankle plantar-flexors. These results show that increasing target stiffness in the knee elevates forces of agonist and antagonist muscles of the knee. Another interesting finding is the concomitant increase in the joint stiffness of the hip and ankle with an increase in
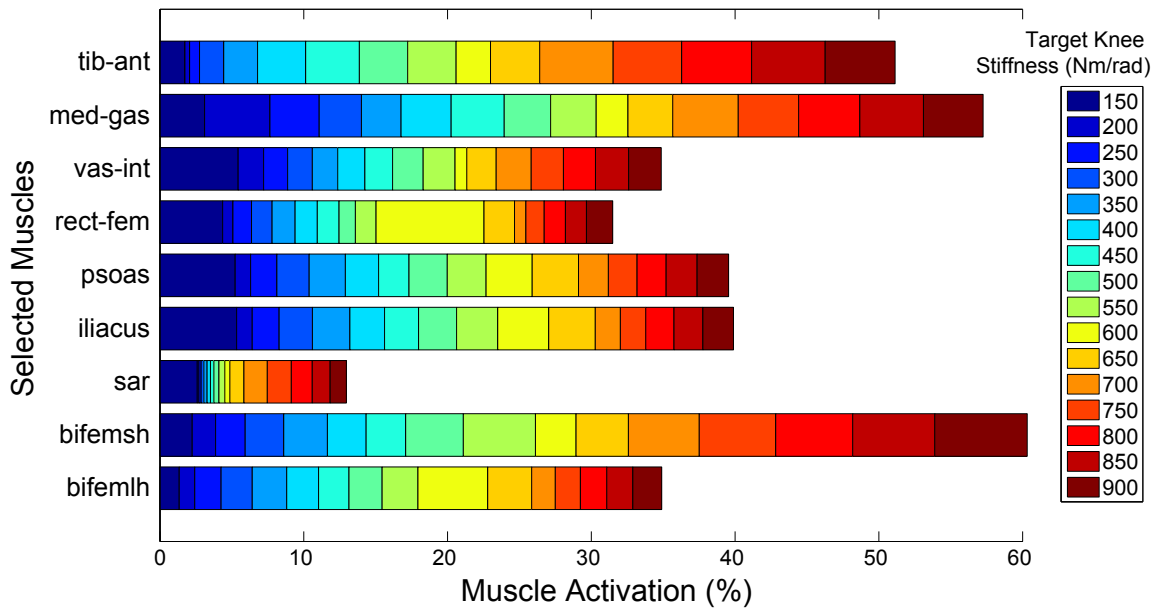
**Figure 4.2:** Muscle activations for increasing levels of target knee stiffness (blue to red). Muscles with greater than 10% activation at the highest stiffness level are shown, including Tibialis Anterior (tib-ant), Medial Gastrocnemius (med-gas), Vastus Intermedius (vas-int), Rectus Femoris (rect-fem), Psoas Major (psoas), Sartorius (sar), Short Head Biceps Femoris (bifemsh), and Long Head Biceps Femoris (bifemlh) muscles.
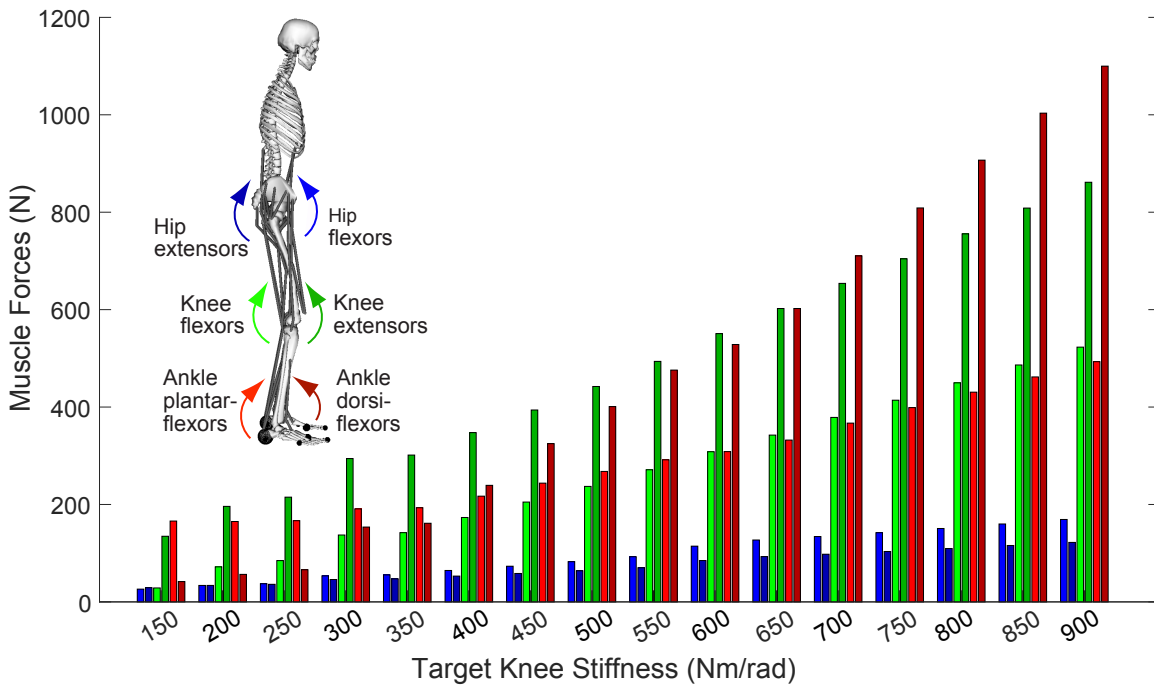


**Figure 4.3:** Average muscle force versus target knee stiffness for the hip flexors (light blue), hip extensors (dark blue), knee flexors (light green), knee extensors (dark green), ankle plantar-flexors (light red), and ankle dorsi-flexors (dark red).

the knee stiffness. Highest target stiffness of the knee was 900 Nm/rad in which maximum muscle activation where 60%. Figure 4.4 presents measured stiffness of the hip and ankle in red and blue, respectively. This plot suggests that increasing the target knee stiffness to 900 Nm/rad would result in 625 and 552 Nm/rad stiffnesses in the hip and ankle.
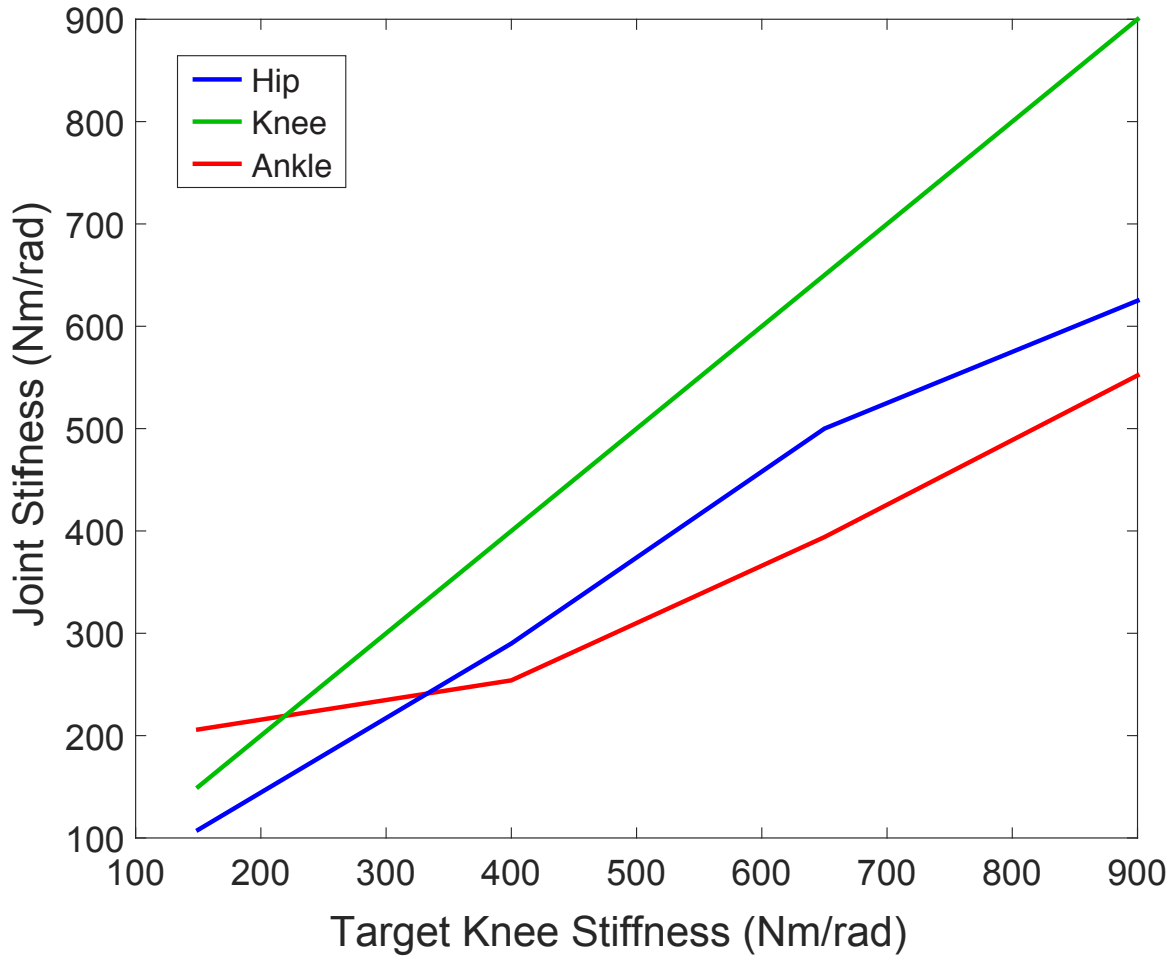


**Figure 4.4:** Hip (blue), Knee (green), and ankle (red) stiffness versus target knee stiffness.

We also validated the knee stiffness by measuring it with the analytical method for both models with Hill-type muscles and model with *SRSMuscles* after optimization to see if the knee stiffness hits the target stiffness. Figure 4.5 demonstrates stiffness of the model with Hill-type muscles in blue and *SRSMuscles* in red. Our finding shows that the measured stiffness in the knee matches the target stiffness set to the knee, in optimization, for the model with *SRSMuscles*. On the other hand, the model with Hill-type muscles demonstrates less measured stiffness compared to the target stiffness.
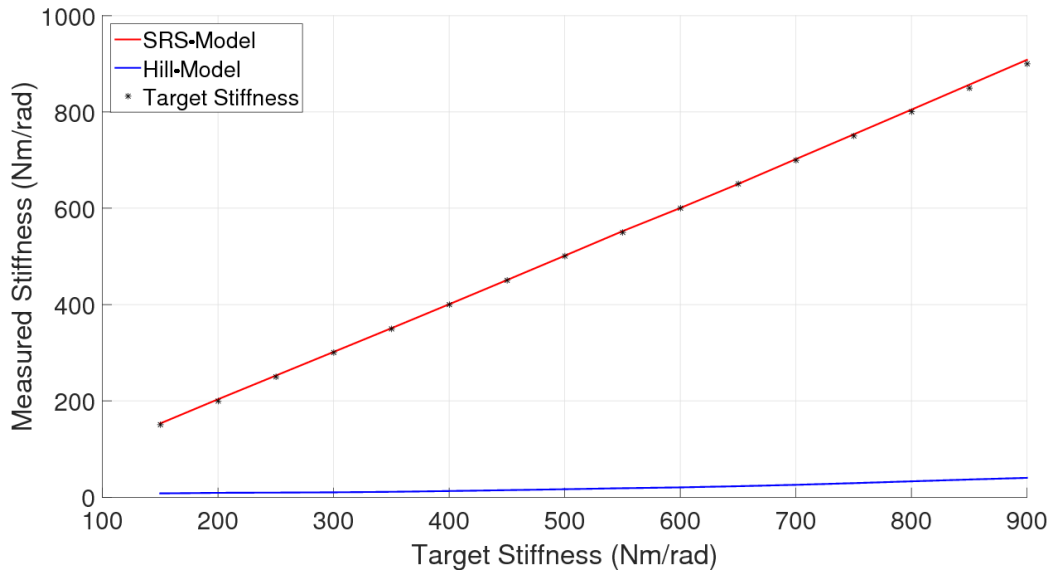
**Figure 4.5:** Knee stiffness was measured directly using the analytical method for the model with Hill-type muscles (blue) and the model with *SRSMuscles* (red). Asterisks denote the target stiffness at each level.

## 4.5 Discussion

### 4.5.1 Verification of the Knee Stiffness

The *SRSMuscle* model was implemented into OpenSim to imrpove the realism of joint stiffness in the model. To test stiffness range in our model, we compared it to experimental data reported in [52]. To this end, we chose a set of target knee flexion torques and calculated the minimum activations to achieve this torque in the knee. Our findings show that the model with *SRSMuscle* at 16 degrees of knee flexion has closer stiffness to experimental data which is taken from [52] while stiffness in Hill-type muscle model is highly underestimated. There is some descrepancy in our model for knee stiffness compared to the experimental data. Stiffness in the model with *SRSMuscle* is underestimated for extension torques, while it is a bit more stiff for flexion torques. We believe these errors in stiffness in our model are due to a different number of muscles and the muscle model, compared to the paper. Optimization would result in a different set of muscle forces that can cause differences in the stiffness of the joint.

### 4.5.2 Measured Stiffness of Knee vs. Target Stiffness

Measured stiffness using the analytical method denotes actual stiffness of the model during simulation. Measured stiffness of the knee for both models (model with Hill-type and SRSMuscles) is plotted in Figure 4.5 against target stiffness. The SRS model has a stiffness in the knee, that matches the target stiffness, which was set in optimization. However, the model with the Hill-type muscles provides less stiffness. This is

because of underestimated stiffness of each Hill-type muscle, which results in a huge error in the stiffness of corresponding joint.

### 4.5.3   Co-activation of the Muscle Groups

Our results (Figure 4.2, Figure 4.3) demonstrate some higher activation in the agonist and antagonist muscles of the knee, while the knee stiffness is increased. Both knee flexors and extensors reached higher muscle activations and forces in higher knee stiffnesses. We started from 150 Nm/rad because this is almost the minimum stiffness which is measured in the knee while the model is optimized to stand with the minimum possible activations. We continued to increase target stiffness of the knee until the maximum muscle activation reached 60%. However, the muscle activation can get as far as 100%, it might cause some injuries to muscle fibers and is not in the physiological range which muscle acts in. Though, muscle damage can happen due to high active muscle strain [33], muscle strains due to excessive tension in musculotendon unit is a general agreement [20]. This excessive tension can happen in higher activation of the muscle.

Increasing target knee stiffness not only increases activations of agonist and antagonist muscles in the knee, but also the same thing happened in the hip and the ankle which caused higher stiffness in those joints (Figure 4.4). This might suggest that increasing the stiffness of one joint in isolation is not possible mainly due to bi-articular muscles. For instance, the Med-Gas muscle is a bi-articular muscle coupled to both the knee and the ankle joints. Increasing the knee stiffness would increase activation of this muscle. Therefore, more activation is needed in the ankle dorsi-flexion muscle group to preserve model's stability (Med-Gas is a muscle connected to the back of the ankle and provides plantar flexion). Hence, Tib-Ant provides higher activation. This results in higher forces in the ankle plantar-flexion and ankle dorsi-flexion muscle groups and higher ankle stiffness, while only the knee stiffness is targeted. The same circumstance happens in the hip and results in higher hip stiffness.

Given the new patterns of muscle co-activation in stance that were found as a result of our static optimization simulations and the realistic levels of knee stiffness elicited in the model, we are interested in assessing how these factors affect postural stability of the model, which is the focus of the next chapter.

# Chapter 5

# Postural Stability

Our new formulation of static optimization provides the ability to encourage co-activation of agonist and antagonist muscles. Our new *SRSMuscle* model in OpenSim permits us to simulate muscles with accurate intrinsic stiffness. In this chapter, we apply these new modeling technique to assess the main scientific hypothesis of the thesis. We hypothesized that higher joint stiffness will lead to higher postural stability; therefore, it would be beneficial to investigate the stability of the model under this new criterion. In this chapter, we will examine the effect of muscle co-activation on postural stability of a standing model under different perturbations.

In the method section, the model configuration and simulation environment are described. Also, the way in which the stability of the model is measured with a stability index and overall stability is described. These stability metrics allow us to determine the stability of the model and provide a means to compare the stability of one model configuration against others. The results section compares the stability of the base model (model with minimum activations and minimum knee stiffness) with Hill-type muscles against model with higher stiffness in the knee. The same comparison in model with *SRSMuscle* was made. Results are interpreted and discussed in the discussion section, along with the limitations of this study.

## 5.1 Introduction

The way in which a person stands, i.e. a person's posture, could have an effect on their stability. Previous musculoskeletal simulations studies have suggested that a more crouched posture could lead to a more stable model [63]. They tested stability under four different postures of 1, 16, 30, and 45 degrees of flexion in the knee. Their study confirms that a model has higher stability at more degrees of knee flexion. Though, a model with 30 degrees of flexion have higher stability. In this study, we explore an alternative question: does the intrinsic stiffness of muscles and the pattern of muscle recruitment significantly affect one's postural stability. We use a similar simulation framework as [63], and the model configuration with a neutral 16 degrees of knee flexion. This model configuration was chosen instead of the model with a crouched stance (30 or 45 degrees in the knee) because it is a natural amount of knee flexion for relaxed standing. It is feasible to choose this level of mild crouch stance for training of people with impaired stability, such as people with Parkinson or older adults with poor balance.

The postural stability of the model is expected to increase by increasing the stiffness of the knee. This high stability could be the result of more stable and stiffer knee against perturbations. Results from [16] and our results from chapters 3 and 4 provided sufficient evidence that higher stiffness at joint would lead to higher co-activation of corresponding muscles. Therefore, higher co-activation was achieved by increasing co-activation of agonist and antagonist muscles of this joint. The intrinsic stiffness of muscle, due to SRS, could play an important role in postural stability. Standard musculoskeletal models, that use Hill-type muscles, should have less stability under perturbations due to lack of intrinsic stiffness, as compared to a model that benefits from SRS. Hence, a new model with the SRS feature is needed to enable the experiment. In the method section, we will describe the creation and setup steps of two models (one with Hill-type muscles, and another with *SRSMuscles*) and will study the following conditions: 1) Stability of a model with Hill-type muscles with and without co-activation, and 2) Stability of a model with *SRSMuscles* with and without co-activation.

## 5.2    Methods

### 5.2.1    HILL-Model and SRS-Model

Model which has been described in the lower extremity model section in chapter 2 was used with a posture determined by optimization. To find the posture, the knee angle was fixed at 16 degrees, and an optimization was performed to calculate the angles of the other joints (coordinates). To this end, the objective was to minimize the forces to keep the model upright and to put center-of-mass (COM) and center-of-pressure (COP) of the model close to the center of the foot. The residual force in the pelvis was constrained to zero. Convergence tolerance and constraint tolerance were 1e-14 and 1e-4 respectively. Inverse dynamics was used in the objective function to determine the forces that were being minimized. This optimization provided values for joint coordinates to be used as initial conditions in the rest of the study for following coordinates: pelvis, hip, ankle, and subtalar joint. Coordinate values are list in Table 5.1.

Using these initial values for coordinates along with Hill-type muscles provided the basic model for posture simulations, which we will refer to it as HILL-Model. Furthermore, these initial posture is used in combination with *SRSMuscle* that we will refer to it as SRS-Model.

### 5.2.2    Base Model Configuration

Base HILL-Model was defined as follows. Minimum activations were calculated to keep the model stationary and the muscles in the HILL-Model are initialized with these activations. We will refer to this model configuration as the base HILL-Model and to the stability of this model as the base HILL-Model stability. Base SRS-Model and its stability were defined in the same way. We collected forces, fiber lengths, and optimal fiber lengths from Hill-type muscles. Then we initialized each muscle of base SRS-Model as described

|  | Value (degrees) |
|---|---|
| Pelvis | Tilt = -1.2 |
|  | Rotation = 0 |
| Hip | Flexion = 6.8 |
|  | Adduction = -3 |
|  | Rotation = -2 |
| Knee | Flexion = 16 |
| Ankle | Flexion = 9.31 |
| Subtalar | Rotation = 9.58 |

**Table 5.1:** Initial coordinate values

in section 4.2.1.

### 5.2.3 Co-Activation Model Configurations

We had 16 target stiffnesses in the knee from 150 to 900 Nm/rad which were performed in chapter 4. For each target stiffness a set of muscle activations and consequently a set of muscle forces was calculated which we will refer to these sets by the target stiffness that was used to calculate them. We had the HILL-Model with 16 sets of activations corresponding to 16 levels of target knee stiffness which provides data to test stability HILL-Model with 16 different sets of activations. The muscle forces for each set of activations were then also used for SRS-Model. We used these muscle activation/force sets to initialize muscles in the model when setting up for the stability simulations.

### 5.2.4 Simulation with Perturbation

To test the stability of each model configuration, we shifted the support platform upon which the model was standing and measured how long it took for the model to fall. The support platform was displaced by a smooth step function acting for 0.25 seconds with a magnitude of displacement ranging from -50 to 50 cm (backwards and forwards). The support platform is a square platform that is located under the model, and the model stands in the middle of the platform with contact forces under each foot. To perform stability tests, we used forward simulation with a Runge-Kutta-Merson Integrator with an accuracy of $1 \times 10^{-9}$ and maximum step size of 0.01.

### 5.2.5 Stability Index

For each perturbation the test is performed in the time range of -0.25 to 2 seconds. The perturbation occurs between -0.25 to 0 seconds. For each perturbation, time-to-fall of the model was measured as the time that

it takes the COM of the model to move outside of its BOS. This leads to 16 different time-to-falls under different speeds for each model configuration. Situations with time-to-fall equal to 2 seconds or higher be considered as stable and simulations were terminated. Following previous work [63], we mapped time-to-fall to a numeric stability index as follows:

$$
S = \begin{cases} 0 & T \leq 0 \\ 1 - e^{-T^2} & 0 < T < 2 \\ 1 & T \geq 2 \end{cases} \tag{5.1}
$$

In equation 5.1, S is stability index and T is time-to-fall. Stability index provides a number between zero and one: zero means the model fell immediately, one means model stayed upright for more than two seconds, and for the rest of the simulations, where model falls somewhere between zero and two seconds, the stability index will be greater than zero and less than one.

### 5.2.6  Overall Stability

To measure an overall postural stability across perturbations for a single test, we plotted stability index against perturbation magnitude and measured the area under the curve. This would be the overall stability of the model under all perturbations which leads to a single number that can be used as a measure of the model's Overall Stability (OS) under the specific configuration. Using OS it would be more feasible to study the effect of increased co-activation on both models. Zero OS means a model that falls in all perturbations and higher OS indicates higher stability. Furthermore, using this method makes it easier to make a comparison between the overall stability of the two models (HILL-Model and SRS-Model) when those models are initiated with the same activation sets.

## 5.3  Results

In this section, we will demonstrate stability index as well as the OS change in each model while knee stiffness and muscle co-activation increased. Furthermore, we will compare the stability change in both Hill and SRS-Models in the presence and absence of muscle co-activation.

Figure 5.1 (top) shows the stability index curve against perturbation for base HILL-Model and HILL-Model with 200 to 900 Nm/rad stiffness in the knee with 50 Nm/rad step. Figure 5.1 (bottom) presents the stability index curve for the base SRS-Model and the SRS-Model with a stiffness of 200 to 900 in the knee with 50 Nm/rad step.

Figure 5.2 shows the stability of the HILL-Model (blue) and SRS-Model (red) at the range of 150 to 900 Nm/rad target knee stiffness. This provides the ability to compare the two HILL and SRS-Models with the same amount of co-activation. Overall Stability of both models is increased when target knee stiffness

41
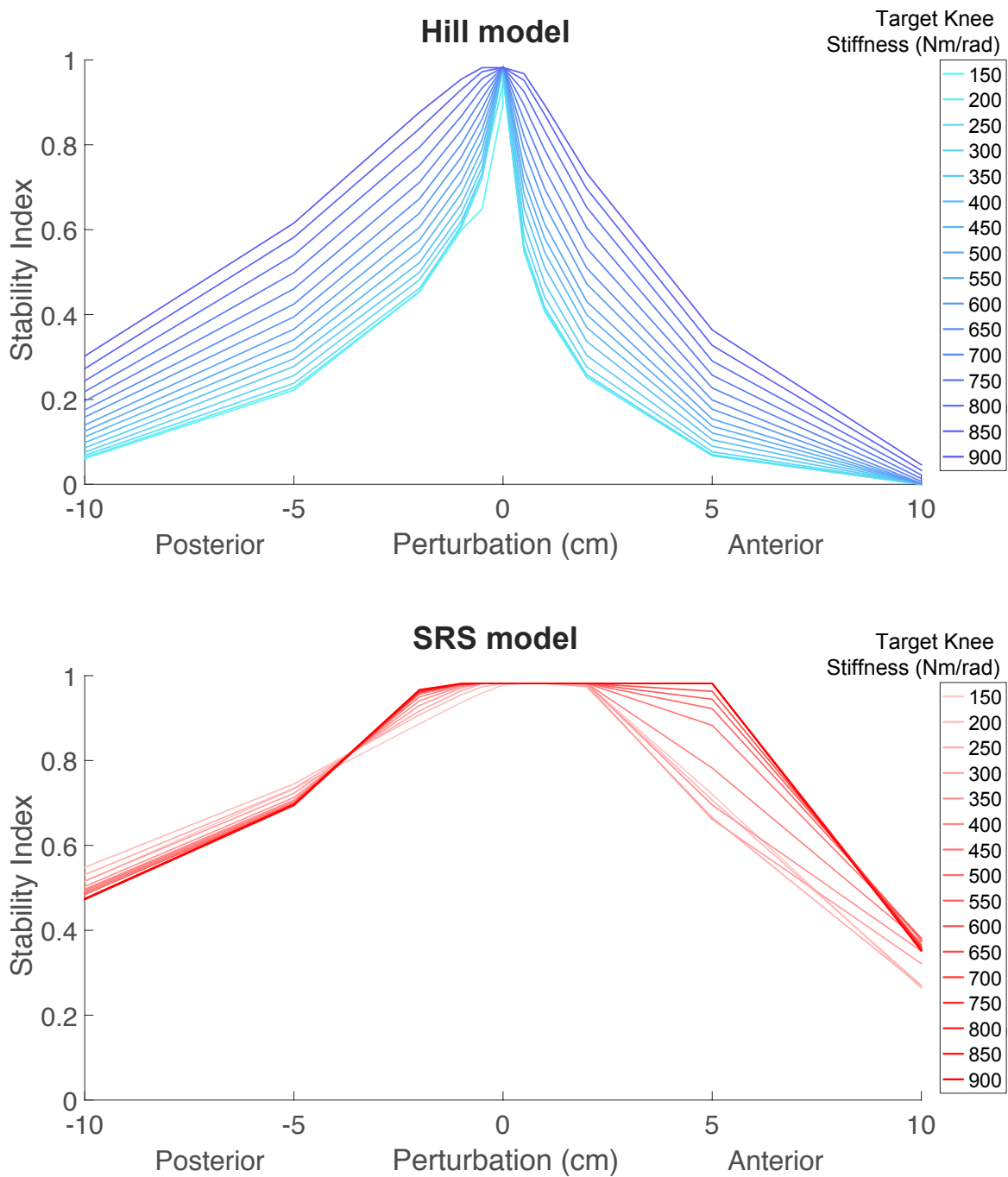
**Figure 5.1:** Stability index versus anteroposterior perturbation magnitude for HILL-Model (top) and SRS-Model (bottom) for increasing levels of target knee stiffness (light to dark lines). Higher stability index is more stable.

increased. While HILL-Models stability increases smoothly by increasing the target stiffness, SRS-Model has a jump in stability between target stiffness of 550 and 600 Nm/rad in the knee.

Overall stability is 0.24 for the base HILL-Model and 0.69 for the HILL-Model with the highest knee stiffness. Base SRS-Model and SRS-Model with 900 Nm/rad stiffness in the knee presents 0.91 and 1.28 OS, respectively. While increasing knee stiffness in HILL-Model from 150 to 900 Nm/rad, almost tripled the overall stability, it has less effect on the SRS-Model (overall stability increased 40% by increasing knee stiffness from 150 to 900 Nm/rad).
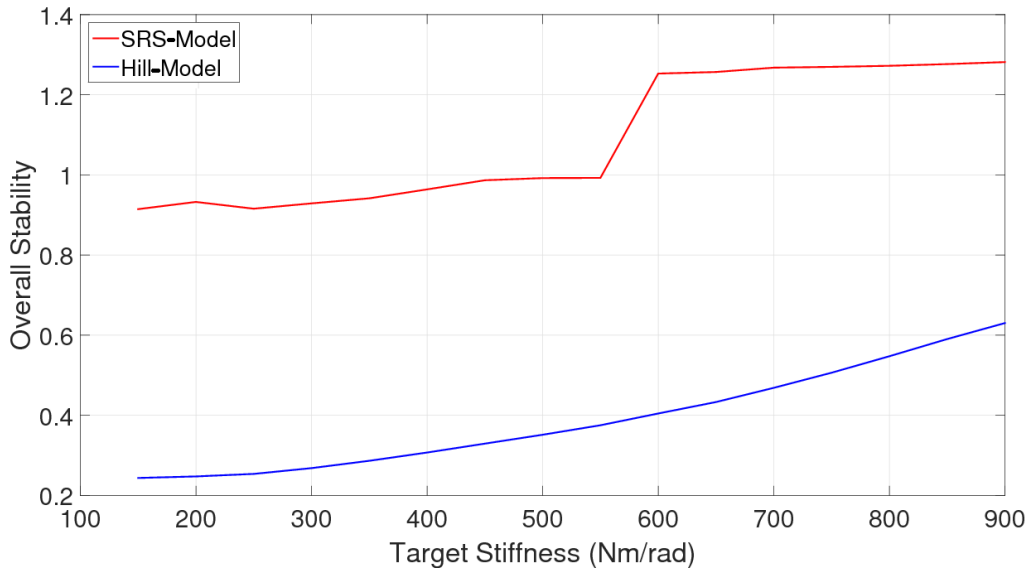


**Figure 5.2:** Overall stability plotted for all 16 levels of target knee stiffness (ranging from 150 to 900 Nm/rad) for the HILL-Model (blue) and the SRS-Model (red).

## 5.4 Discussion

Our simulation results demonstrate that both intrinsic stability due to short range stiffness of the muscle and joint stiffness elicited by muscle co-activation contribute to the stability of the standing posture. The HILL-Model exhibited a smooth increase in overall stability across target knee stiffness levels. The SRS-Model, however, exhibited a large jump in the curve between 600 and 650 Nm/rad for target knee stiffness (Figure 5.2). By examining the muscle activations for each target stiffness, we found a shift in recruitment strategy whereby the Rectus Femoris muscle activation increased substantially between the 550 and 600 Nm/rad target levels (Figure 4.2). Rectus Femoris is a bi-articular knee flexor and therefore this result suggests that an increase in this muscle had a particularly important effect on postural stability, which is consistent with previous work suggesting bi-articular muscles may play an important stabilizing role [9].

Our goal was to investigate effect of intrinsic stability through simulation, but the absence of reflexes and postural responses in our model prevents us to extend this approach and investigate the overall stability that

includes responses. There are previous studies on including reflexes into simplified posture models and tuning velocity and length gains to match experimental data [56]. However, due to delays in responses from the nervous system, intrinsic stability still plays an important role in stabilizing the body. It becomes even more important when responses are impaired or more delayed due to the aging or other reasons. Incorporating reflex and postural responses into a biomechanical simulation of support platform perturbations is planned as future work.

# Chapter 6

# Conclusion & Future Work

This thesis described a novel formulation for static optimization to encourage muscle co-activation, as well as a new muscle model to capture the intrinsic stiffness of muscle fibers. Moreover, the new muscle model was integrated into the lower extremity model, which was used in forward simulations for assessing postural stability. This chapter will give an overview of the thesis contributions and highlight potential directions for future work.

## 6.1 Contributions

The contributions of this thesis can be summarized into four main areas: 1) a new formulation for static optimization, 2) development of a new muscle model, *SRSMuscle* in OpenSim, 3) implementation of a new technique to measure joint stiffness in OpenSim, and 4) a detailed analysis of the postural stability of a musculoskeletal model with/without muscle co-activation and with/without instrinsic muscle stiffness.

### 6.1.1 Static Optimization

Static optimization takes the results of Inverse Dynamics (ID) — net joint torques — as an input and distributes them among the muscles by minimizing an objective function subject to some constraints. Net joint torque and maximum muscle forces are usually equality and non-equality constraints of the problem, respectively. The objective function could be muscle forces, muscle stresses (physiological energy), or muscle activations. Regardless of the objective function selection, traditional static optimization does not estimate muscle forces correctly in the presence of the muscle co-activation. This is because it spreads net joint moment among agonist muscles, while minimizing forces of antagonist muscles.

Our formulation of static optimization adds a new equality constraint — the joint stiffness — in order to elicit muscle co-activation. Besides, it allows a controlled level of co-activation among muscles by controlling the stiffness of the joint, rather than requiring manual prescription of co-activation level. This new formulation is a general purpose formulation that can be used by other researchers interested in analyzing human movmeents that include muscle co-activation. It can be applied to a multi-joint model optimization and eliminates the need for electromyography measurements to inform how much to spread joint torques among muscles in the presence of co-activation.

### 6.1.2 *SRSMuscle* Model

Muscles are responsible for producing motion in the human body by applying forces to bones that, in turn, cause joints to move. Hence, for physics based simulation purposes, an accurate muscle model is necessary. Hill-type muscle model is one of the models that has been introduced and implemented in OpenSim, and widely used in a lot of studies. However, this muscle model, has been known to underestimate the stiffness of muscle. We created a new muscle model that captures intrinsic short range stiffness of a physiological muscle, and can be used in posture simulations. The new muscle model is an extension to the *PathSpring* force model in OpenSim. This new muscle model is sufficient to be used in the stance simulations and is integrated into the lower extremity model.

We evaluated this model using the experimental setup protocol from [52]. Knee muscles were optimized to produce extension torque ranging from -40 to 60 Nm/rad and the stiffness of the joint was calculated and compared to model in [52]. Despite differences between our model and the model in [52], the knee stiffness found with our *SRSMuscle* model corresponded well with experimental data.

### 6.1.3 Joint Stiffness

Joint stiffness is the extent to which a joint can resist an applied force. To date, OpenSim does not provide a built-in method to measure the joint stiffness. The stiffness of the joint can be measured both numerically and analytically. Since both methods could be computationally efficient in different situations, we developed both methods and verified our implementation by applying it to a simplified model with a single joint and one to four actuators. Since, moment arms and moment arms derivatives are required for the analytical approach, this approach is efficient when the posture of the model is constant and only the joint torques are being changed. On the other hand, the numerical method is computationally efficient when the posture of the model is constantly changing. That is the case, because numerical approach, to measure the joint stiffness, does not require the moment arm derivative as a direct input.

### 6.1.4 Posture Simulations

Postural stability, the ability to stand without falling, could be affected by many internal (e.g. sway, breathing, etc.) and external factors (perturbations). In this thesis, we hypothesized that higher co-activation among leg muscles could lead to higher stability. We had some obstacles in our way before testing this hypothesis. Our first three contributions in this thesis dealt with these obstacles to provide the ability to investigate this assumption. In the last part of this thesis, we created an environment to test stance stability. To this end, we shifted platform beneath the model with different amplitudes and measured time-to-fall for each case. Time-to-falls are converted to stability indexes. This gave us ability to compare total stability of different model configurations (for instance different co-activation levels). Our results from this section supported our hypothesis that higher co-activation and joint stiffness can lead to higher postural stability.

## 6.2 Future Work

There are multiple possible research directions that could improve our contributions in this thesis. In this section, we will discuss a few of the limitations in our model and approach. Further studies in these areas could be a huge enhancement to our work.

### 6.2.1 *SRSMuscle* Model

The *SRSMuscle* that has been discussed in this thesis is sufficient to be used in situations of static equilibrium. This model has sufficient stiffness that enables us to use it for the purpose of this thesis. However, it is a simple model for a muscle to be used in stance simulations and lacks other features of a promising muscle model. An improvement to this model would be combining it with the Hill-type muscle model, which inherits its features from both models. Such a muscle would function like a Hill-type muscle while benefiting from *SRSMuscle* stiffness.

### 6.2.2 Reflex Controls

Reflex control is an impulse that is issued by the central nervous system to a muscle in order to maintain a normal reflex action. Our model — the lower extremity model — lacks reflex controls that makes it unstable when the reflexes are needed (for instance, when a big perturbation is applied to the model). Currently, the model uses constant controls for muscles, which is sufficient to measure the intrinsic stability of the body. But, for complicated tasks such as walking, the model would benefit from the reflex controllers. Hence, adding these controllers to the model, could improve the stability of the model in both standing and walking tasks.

### 6.2.3 Gait Simulations

In this thesis, we used the *SRSMuscle* model to capture the short range stiffness property of muscle tissue. This is applicable to the stance because the muscles are in a static equilibrium and the length of the fibers are not changing. In a circumstance like gait, when the muscle fiber length is constantly changing, the degree to which the short range stiffness persists is not clear. Hence, the way in which the short range stiffness can affect stability during walking is an open question. A further study is needed to answer this question and could be performed as an extension of our stance perturbation simulation environment.

## 6.3 Conclusion

Our original hypothesis, stated that the higher muscle co-activation leads to the higher stance intrinsic stability. In order to investigate this hypothesis, we needed a method to perform the static optimization in

the presence of the co-activation. We have presented the development of new optimization formulation, which employs the joint stiffness as an equality constraint to encourage co-activation among agonist and antagonist muscles. Additionally, a new method was presented to measure joint stiffness.

The Hill-type muscle model was not sufficient for this purpose as a result of its underestimated stiffness. Accordingly, the *SRSMuscle* model was implemented to conquer this issue. This model was used along with the new optimization formulation to acquire different level of muscle co-activation for the model. Our results showed that there is a correlation between co-activation of muscles and stance stability. Higher levels of co-activation presented higher stability. Additionally, our results demonstrated that using the *SRSMuscle* model introduces more stability compared to the Hill-type muscle model, when a same pattern of muscle activations is used for the both muscle models.

# REFERENCES

[1] R Baratta, M Solomonow, BH₋ Zhou, D Letson, R Chuinard, R D'ambrosia, et al. Muscular coactivation the role of the antagonist musculature in maintaining knee stability. *The American journal of sports medicine*, 16(2):113–122, 1988.

[2] Jeffrey T Bingham, Julia T Choi, and Lena H Ting. Stability in a frontal plane model of balance requires coupled changes to postural configuration and neural feedback control. *Journal of neurophysiology*, 106(1):437–448, 2011.

[3] Richard A Brand, Douglas R Pedersen, and James A Friederich. The sensitivity of muscle force predictions to changes in physiologic cross-sectional area. *Journal of biomechanics*, 19(8):589–596, 1986.

[4] Ian E Brown and Gerald E Loeb. A reductionist approach to creating and using neuromusculoskeletal models. In *Biomechanics and neural control of posture and movement*, pages 148–163. Springer, 2000.

[5] Stephen C Cannon and George I Zahalak. The mechanical behavior of active human skeletal muscle in small oscillations. *Journal of biomechanics*, 15(2):111–121, 1982.

[6] Germana Cappellini, Yuri P Ivanenko, Nadia Dominici, Richard E Poppele, and Francesco Lacquaniti. Motor patterns during walking on a slippery walkway. *Journal of neurophysiology*, 103(2):746–760, 2010.

[7] Norman V Carroll, Patricia W Slattum, and Fred M Cox. The cost of falls among the community-dwelling elderly. *Journal of Managed Care Pharmacy*, 11(4):307–316, 2005.

[8] Miguel Christophy, Nur Adila Faruk Senan, Jeffrey C Lotz, and Oliver M OReilly. A musculoskeletal model for the lumbar spine. *Biomechanics and modeling in mechanobiology*, 11(1-2):19–34, 2012.

[9] Ashley E Clark, Ajay Seth, and Jeffrey A Reinbolt. Biarticular muscles influence postural responses: implications for treatment of stiff-knee gait. XIII International Symposium on Computer Simulation in Biomechanics. Leuven, Belgium, 2011.

[10] JJ Collins. The redundant nature of locomotor optimization laws. *Journal of biomechanics*, 28(3):251–267, 1995.

[11] Roy D Crowninshield and Richard A Brand. A physiologically based criterion of muscle force prediction in locomotion. *Journal of biomechanics*, 14(11):793–801, 1981.

[12] Lei Cui, Eric J Perreault, Huub Maas, and Thomas G Sandercock. Modeling short-range stiffness of feline lower hindlimb muscles. *Journal of biomechanics*, 41(9):1945–1952, 2008.

[13] CJ De Luca and B Mambrito. Voluntary control of motor units in human antagonist muscles: coactivation and reciprocal activation. *Journal of neurophysiology*, 58(3):525–542, 1987.

[14] Scott L Delp, Frank C Anderson, Allison S Arnold, Peter Loan, Ayman Habib, Chand T John, Eran Guendelman, and Darryl G Thelen. Opensim: open-source software to create and analyze dynamic simulations of movement. *Biomedical Engineering, IEEE Transactions on*, 54(11):1940–1950, 2007.

[15] Scott L Delp, J Peter Loan, Melissa G Hoy, Felix E Zajac, Eric L Topp, and Joseph M Rosen. An interactive graphics-based model of the lower extremity to study orthopaedic surgical procedures. *Biomedical Engineering, IEEE Transactions on*, 37(8):757–767, 1990.

[16] Yasin Y Dhaher, Anastasios D Tsoumanis, Timothy T Houle, and William Z Rymer. Neuromuscular reflexes contribute to knee stiffness during valgus loading. *Journal of neurophysiology*, 93(5):2698–2709, 2005.

[17] Ahmet Erdemir, Scott McLean, Walter Herzog, and Antonie J van den Bogert. Model-based estimation of muscle forces exerted during movements. *Clinical biomechanics*, 22(2):131–154, 2007.

[18] Centers for Disease Control and Prevention. Cost of injery report. `http://www.cdc.gov/injury/wisqars/`. [online; Accessed August 2015.].

[19] Canadian Institute for Health Information. Measuring up. a yearly report on how ontario's health system is performing. Technical report, 2009.

[20] William E Garrett, Marc R Safran, Anthony V Seaber, Richard R Glisson, Beth M Ribbeck, et al. Biomechanical comparison of stimulated and nonstimulated skeletal muscle pulled to failure. *The American journal of sports medicine*, 15(5):448–454, 1987.

[21] U Glitsch and W Baumann. The three-dimensional determination of internal loads in the lower extremity. *Journal of biomechanics*, 30(11):1123–1131, 1997.

[22] S Hagood, M Solomonow, R Baratta, BH Zhou, and R D'ambrosia. The effect of joint velocity on the contribution of the antagonist musculature to knee stiffness and laxity. *The American Journal of Sports Medicine*, 18(2):182–187, 1990.

[23] Z Hasan. Optimized movement trajectories and joint stiffness in unperturbed, inertially loaded movements. *Biological cybernetics*, 53(6):373–382, 1986.

[24] Walter Herzog. Sensitivity of muscle force estimations to changes in muscle input parameters using nonlinear optimization approaches. *Journal of biomechanical engineering*, 114(2):267–268, 1992.

[25] Neville Hogan. Adaptive control of mechanical impedance by coactivation of antagonist muscles. *Automatic Control, IEEE Transactions on*, 29(8):681–690, 1984.

[26] Katherine RS Holzbaur, Wendy M Murray, and Scott L Delp. A model of the upper extremity for simulating musculoskeletal surgery and analyzing neuromuscular control. *Annals of biomedical engineering*, 33(6):829–840, 2005.

[27] Fay B Horak. Postural orientation and equilibrium: what do we need to know about neural control of balance to prevent falls? *Age and ageing*, 35(suppl 2):ii7–ii11, 2006.

[28] Xiao Hu, Wendy M Murray, and Eric J Perreault. Muscle short-range stiffness can be used to estimate the endpoint stiffness of the human arm. *Journal of neurophysiology*, 105(4):1633–1641, 2011.

[29] Chand T John, Frank C Anderson, Jill S Higginson, and Scott L Delp. Stabilisation of walking by intrinsic muscle properties revealed in a three-dimensional muscle-driven simulation. *Computer methods in biomechanics and biomedical engineering*, 16(4):451–462, 2013.

[30] Kenton R Kaufman, K-N Au, William J Litchy, and EYS Chao. Physiological prediction of muscle forcesii. application to isokinetic exercise. *Neuroscience*, 40(3):793–804, 1991.

[31] Francesco Lacquaniti and Claudio Maioli. Anticipatory and reflex coactivation of antagonist muscles in catching. *Brain research*, 406(1):373–378, 1987.

[32] WD Leslie, LM Lix, GS Finlayson, CJ Metge, SN Morin, and SR Majumdar. Direct healthcare costs for 5 years post-fracture in canada. *Osteoporosis International*, 24(5):1697–1705, 2013.

[33] Richard L Lieber and Jan Friden. Muscle damage is not a function of muscle force but active muscle strain. *Journal of Applied Physiology*, 74(2):520–526, 1993.

[34] Dong C Liu and Jorge Nocedal. On the limited memory bfgs method for large scale optimization. *Mathematical programming*, 45(1-3):503–528, 1989.

[35] John E Lloyd, Ian Stavness, and Sidney Fels. Artisynth: a fast interactive biomechanical modeling toolkit combining multibody and finite element simulation. In *Soft tissue biomechanical modeling for computer assisted surgery*, pages 355–394. Springer, 2012.

[36] Diane Manchester, Marjorie Woollacott, Niki Zederbauer-Hylton, and Oscar Marin. Visual, vestibular and somatosensory contributions to balance control in the older adult. *Journal of Gerontology*, 44(4):M118–M127, 1989.

[37] J McIntyre, FA Mussa-Ivaldi, and E Bizzi. The control of stable postures in the multijoint arm. *Experimental brain research*, 110(2):248–264, 1996.

[38] I Melzer, N Benjuya, and J Kaplanski. Age-related changes of postural control: effect of cognitive tasks. *Gerontology*, 47(4):189–194, 2001.

[39] Matthew Millard, Thomas Uchida, Ajay Seth, and Scott L Delp. Flexing computational muscle: modeling and simulation of musculotendon dynamics. *Journal of biomechanical engineering*, 135(2):021005, 2013.

[40] Koutatsu Nagai, Minoru Yamada, Kazuki Uemura, Yosuke Yamada, Noriaki Ichihashi, and Tadao Tsuboyama. Differences in muscle coactivation during postural control between healthy older and young adults. *Archives of gerontology and geriatrics*, 53(3):338–343, 2011.

[41] Government of Canada. Canadians in context - aging population. `http://well-being.esdc.gc.ca/misme-iowb/.3ndic.1t.4r@-eng.jsp?iid=33`. [Online; accessed Feb-2016].

[42] Government of Canada. Actions for seniors. Technical report, 2014.

[43] Public Health Agency of Canada. Seniors'falls in canada. Technical report, 2014.

[44] Department of Economic and Social Affairs. Population Division. World population Aging 1950-2050. `http://www.un.org/esa/population/publications/worldageing19502050/pdf/80chapterii.pdf`. [Online; accessed Jan-2016].

[45] National Institute on Aging. An Aging World: US Department of Health and Human Service. Technical report, 2009.

[46] National Institute on Aging. Humanity's aging: Us department of health and human service. Technical report, 2011.

[47] Matthew C O' Neill, Leng-Feng Lee, Susan G Larson, Brigitte Demes, Jack T Stern, and Brian R Umberger. A three-dimensional musculoskeletal model of the chimpanzee (pan troglodytes) pelvis and hind limb. *Journal of Experimental Biology*, 216(19):3709–3723, 2013.

[48] Christopher S Pan, Sharon Chiou, Tsui-Ying Kau, Amit Bhattacharya, and Doug Ammons. Effects of foot placement on postural stability of construction workers on stilts. *Applied ergonomics*, 40(4):781–789, 2009.

[49] J Parkkari, P Kannus, M Palvanen, A Natri, J Vainio, H Aho, I Vuori, and M Järvinen. Majority of hip fractures occur as a result of a fall and impact on the greater trochanter of the femur: a prospective controlled hip fracture study with 206 consecutive patients. *Calcified Tissue International*, 65(3):183–187, 1999.

[50] DR Pedersen, RA Brand, C Cheng, and JS Arora. Direct comparison of muscle force predictions using linear and nonlinear programming. *Journal of Biomechanical Engineering*, 109(3):192–199, 1987.

[51] Eric J Perreault, Robert F Kirsch, and Patrick E Crago. Effects of voluntary force generation on the elastic components of endpoint stiffness. *Experimental Brain Research*, 141(3):312–323, 2001.

[52] Serge Pfeifer, Heike Vallery, Michael Hardegger, Robert Riener, and Eric J Perreault. Model-based estimation of knee stiffness. *Biomedical Engineering, IEEE Transactions on*, 59(9):2604–2612, 2012.

[53] Saskatchewan Health Population Health Branch. Falls injuries among saskatchewan seniors, 1992/93 to 1997/98: Implications for prevention. Technical report, 2002.

[54] Peter MH Rack and DR Westbury. The short range stiffness of active mammalian muscle and its effect on mechanical properties. *The Journal of physiology*, 240(2):331, 1974.

[55] H Röhrle, R Scholten, C Sigolotto, W Sollbach, and H Kellner. Joint forces in the human pelvis-leg skeleton during walking. *Journal of Biomechanics*, 17(6):409–424, 1984.

[56] Seyed A Safavynia and Lena H Ting. Long-latency muscle activity reflects continuous, delayed sensorimotor feedback of task-level and not joint-level error. *Journal of neurophysiology*, 110(6):1278–1290, 2013.

[57] Alice C Scheffer, Marieke J Schuurmans, Nynke Van Dijk, Truus Van Der Hooft, and Sophia E De Rooij. Fear of falling: measurement strategy, prevalence, risk factors and consequences among older persons. *Age and ageing*, 37(1):19–24, 2008.

[58] Ajay Seth and Scott L. Delp. Does crouch improve postural stability? ISB, 2011.

[59] Ajay Seth, Michael Sherman, Peter Eastman, and Scott Delp. Minimal formulation of joint motion for biomechanisms. *Nonlinear dynamics*, 62(1-2):291–303, 2010.

[60] Michael A Sherman, Ajay Seth, and Scott L Delp. Simbody: multibody dynamics for biomedical research. *Procedia Iutam*, 2:241–261, 2011.

[61] Laura B Shrestha. Population aging in developing countries. *Health affairs*, 19(3):204–212, 2000.

[62] Allan M Smith. The coactivation of antagonist muscles. *Canadian journal of physiology and pharmacology*, 59(7):733–747, 1981.

[63] Ian Stavness, Vaughn Friesen, and Ajay Seth. Musculoskeletal simulation of posture perturbations in opensim. World Congress of Biomechanics, 2014.

[64] Judy A Stevens, Phaedra S Corso, Eric A Finkelstein, and Ted R Miller. The costs of fatal and non-fatal falls among older adults. *Injury prevention*, 12(5):290–295, 2006.

[65] Laura A Talbot, Robin J Musiol, Erica K Witham, and E Jeffery Metter. Falls in young, middle-aged and older community dwelling adults: perceived cause, environmental factors and injury. *BMC Public Health*, 5(1):1, 2005.

[66] Andreas Wächter and Lorenz T Biegler. On the implementation of an interior-point filter line-search algorithm for large-scale nonlinear programming. *Mathematical programming*, 106(1):25–57, 2006.

[67] Heiko Wagner and Reinhard Blickhan. Stabilizing function of skeletal muscles: an analytical investigation. *Journal of Theoretical Biology*, 199(2):163–179, 1999.

[68] ME Wiktorowicz, R Goeree, A Papaioannou, Jonathan D Adachi, and E Papadimitropoulos. Economic implications of hip fracture: health service use, institutional care and cost in canada. *Osteoporosis International*, 12(4):271–278, 2001.

[69] Yoshihiko Yamazaki, Masataka Suzuki, Tetsuo Ohkuwa, and Hiroshi Itoh. Coactivation in arm and shoulder muscles during voluntary fixation of a single joint. *Brain research bulletin*, 59(6):439–446, 2003.

# Appendix A

# List of Muscles That Are Used in the Lower Extremity Model

| Muscle name | Maximum Force (N) | Optimal fiber length (m) | Acting group(s) |
|---|---|---|---|
| Gluteus Medius I | 1119 | 0.0535 | Hip Abduction Hip Flexion Hip Internal Rotation |
| Gluteus Medius II | 873 | 0.0845 | Hip Abduction |
| Gluteus Medius III | 1000 | 0.0646 | Hip Abduction Hip External Rotation Hip Extension |
| Long Head Biceps Femoris | 2700 | 0.109 | Hip Extension Hip Adduction Knee Flexion |
| Short Head Biceps Femoris | 804 | 0.173 | Knee Flexion |
| Sartorius | 156 | 0.52 | Hip Abduction Hip Flexion Knee Flexion |
| Adductor MagnusII | 2343 | 0.121 | Hip Extension Hip Adduction |
| Tensor fasciae latae | 233 | 0.095 | Hip Abduction Hip Flexion Hip Internal Rotation |
| Pectineus | 266 | 0.1 | Hip Flexion Hip Adduction |
| Gracilis | 162 | 0.352 | Hip Flexion Hip Adduction Knee Flexion |
| Gluteus MaximusI | 573 | 0.142 | Hip Abduction Hip Extension |
| Gluteus MaximusII | 819 | 0.147 | Hip Extension |
| Gluteus MaximusIII | 552 | 0.144 | Hip Extension |
| Iliacus | 1073 | 0.1 | Hip Flexion Hip Internal Rotation |
| Psoas Major | 1113 | 0.1 | Hip Flexion Hip Internal Rotation |
| Quadriceps Femoris | 381 | 0.054 | Hip External Rotation |
| Gemellus | 164 | 0.024 | Hip External Rotation |
| Piriformis | 444 | 0.026 | Hip Abduction Hip External Rotation |
| Rectus Femoris | 1169 | 0.114 | Hip Flexion knee Extension |
| Vastus Intermedius | 5000 | 0.107 | knee Extension |
| Medial Gastrocnemius | 2500 | 0.09 | Knee Flexion Ankle Plantar-Flexion |

**Table A.1:** Muscles of the Lower Extremity Model

| Muscle name | Maximum Force (N) | Optimal fiber length (m) | Acting group(s) |
|---|---|---|---|
| Soleus | 4000 | 0.05 | Ankle Plantar-Flexion |
| Tibialis Posterior | 3600 | 0.031 | Ankle Plantar-Flexion |
| Tibialis Anterior | 3000 | 0.098 | Ankle Dorsi-Flexion |
| Erector Spinae | 2500 | 0.12 | Lumbar Extension |
| Internal Abdominal Obliques | 900 | 0.1 | Lumbar Flexion |
| External Abdominal Obliques | 900 | 0.12 | Lumbar Flexion |

# Appendix B

# List of Muscles That Are Used in the Arm Model

| Muscle name | Maximum Force (N) | Optimal fiber length (m) | Acting group(s) |
| --- | --- | --- | --- |
| Long Head Triceps Brachii | 798.52 | 0.134 | elbow extensor |
| Lateral Head Triceps Brachii | 624.3 | 0.1138 | elbow extensor |
| Medial Head Triceps Brachii | 624.3 | 0.1138 | elbow extensor |
| Long Head Biceps Brachii | 624.3 | 0.1157 | elbow flexor |
| Short Head Biceps Brachii | 435.56 | 0.1321 | elbow flexor |
| Brachioradialis | 987.26 | 0.0858 | elbow flexor |

**Table B.1:** Muscles of the Arm Model